Quaternary Research 81 (2014) 339–354

Contents lists available at ScienceDirect

Quaternary Research

journal homepage: www.elsevier.com/locate/yqres

The high-supply, current-dominated continental margin of southeastern South America during the late Quaternary

Hendrik Lantzsch [a,*], Till J.J. Hanebuth [b], Cristiano M. Chiessi [c], Tilmann Schwenk [d], Roberto A. Violante [e]

[a] MARUM — Center for Marine Environmental Sciences and Faculty of Geosciences, University of Bremen, P.O. Box 330 440, 28334 Bremen, Germany
[b] MARUM — Center for Marine Environmental Sciences, University of Bremen, Germany
[c] School of Arts, Sciences and Humanities, University of Sao Paulo, Brazil
[d] MARUM — Center for Marine Environmental Sciences and Faculty of Geosciences, University of Bremen, Germany
[e] Servicio de Hidrografía Naval, Buenos Aires, Argentina

ARTICLE INFO

Article history:
Received 25 April 2013
Available online 6 February 2014

Keywords:
Marine depocenters
Sedimentary pathways
Current control
Source to sink
Southeastern South America
Southwest Atlantic
Water masses
Late Quaternary

ABSTRACT

The continental margin off the La Plata Estuary (SE South America) is characterized by high fluvial sediment supply and strong ocean currents. High-resolution sediment-acoustic data combined with sedimentary facies analysis, AMS-^{14}C ages, and neodymium isotopic data allowed us to reconstruct late Quaternary sedimentary dynamics in relation to the two major sediment sources, the La Plata Estuary and the Argentine margin. Sediments from these two provinces show completely different dispersal patterns. We show that the northward-trending La Plata paleo-valley was the sole transit path for the huge volumes of fluvial material during lower sea levels. In contrast, material from the Argentine margin sector was transported northwards by the strong current system. Despite the large sediment volumes supplied by both sources, wide parts of the shelf were characterized by either persistent non-deposition or local short-term depocenter formation. The location and formation history of these depocenters were primarily controlled by the interplay of sea level with current strength and local morphology. The high sediment supply was of secondary importance to the stratigraphic construction, though locally resulting in high sedimentation rates. Thus, the shelf system off the La Plata Estuary can be considered as a hydrodynamic-controlled end-member.

Introduction

Continental shelf systems off major rivers are usually characterized by a high supply of clastic sediments. As a consequence, deposits on continental shelf and slope are laterally extensive with high accumulation rates (Kuehl et al., 1997; Hübscher et al., 2002; Hanebuth et al., 2011). In contrast, bypassing, winnowing and erosion of sediments, sweeping by persistent unidirectional currents, and redeposition are common processes on shelves dominated by a high-energy oceanographic regime (Flemming, 1981; Ikehara, 1989; Cawthra et al., 2012). The knowledge on the general sedimentary buildup and evolution of these high-energy systems remains sparse due to difficulties in sampling the commonly coarse-grained material. The continental margin off SE South America is characterized by both the highest sediment supply by the La Plata River (Plata hereafter; Depetris and Griffin, 1968; Urien, 1972) as well as strong oceanographic currents (Möller et al., 2008; Palma et al., 2008). The Uruguay and Paraná Rivers, on the one hand, supply a suspended sediment load of 100 Mt yr^{-1} (Milliman and Farnsworth, 2011) to the Plata Estuary and the adjacent continental shelf. The shelf hosts, on the other hand, one of the worldwide strongest current regimes (Gwilliam et al., 1997; Palma et al., 2008). Prior to this study, the resulting late Quaternary stratigraphic architecture and depocenter shifts were virtually unknown.

Although continental margins represent the major sink for terrigenous particles along the source-to-sink pathway from continental interior to the deep sea, the precise routes of sediment transport remain often unknown. For instance, canyons off major rivers are usually suggested to have been the main material conduit during lower sea levels (van Wagoner et al., 1988). At the continental margin off SE South America, sediment pathways during stages of lower sea level are still matter of debate and several possible main transport routes have been proposed in the literature (Lonardi and Ewing, 1971; Urien and Ottmann, 1971; Urien and Ewing, 1974; Urien et al., 1980a,b). These alternative pathways would, however, result in completely different patterns of sediment transit and supply to the continental slope.

Here we use a combination of acoustic profiles and information from sediment cores to unravel the late Quaternary history of the SE South American margin. Reconstructing the formation and lateral migration of main depocenters reveals a comprehensive picture of sediment

* Corresponding author. Fax: +49 421 218 65219.
E-mail address: lantzsch@uni-bremen.de (H. Lantzsch).

0033-5894/$ – see front matter © 2014 University of Washington. Published by Elsevier Inc. All rights reserved.
http://dx.doi.org/10.1016/j.yqres.2014.01.003

distribution and transport pathways during changes in sea level. These deposits also provide valuable information on the export of material to the associated continental slope. Thus, we were able to scrutinize the interaction of high fluvial supply with a strong oceanographic regime on system-wide sedimentation patterns.

Regional settings

Coastal morphology and seafloor physiography

The study area is located off southern Brazil, Uruguay, and northernmost Argentina at approximately 32.5 to 39.5°S (Fig. 1). The shelf width ranges from 130 km off Laguna de Castillos to more than 200 km off Cape San Antonio. The most prominent feature at the coastline is the funnel-shaped Plata Estuary (Fig. 1). In addition, several lagoons developed at the Uruguayan and Brazilian coastlines during Holocene times (e.g., Villwock, 1984; Cordeiro and Lorscheitter, 1994; García-Rodríguez et al., 2004; Fig. 1).

The inner continental shelf off the Uruguayan coast is characterized by an elongated seafloor depression, which represents the Plata paleo-valley (Urien and Ottmann, 1971; Urien and Ewing, 1974; Urien et al., 1980a,b; Laborde, 1999; Cavallotto and Violante, 2005). South of this paleo-valley, the inner shelf shows relicts of complex barrier islands and sand banks that constituted the major morphosedimentary features developed in the region during the post-glacial transgression (Urien and Ewing, 1974; Urien et al., 1980a,b; Parker et al., 2008; Violante et al., 2010).

The outer shelf is characterized by a morphological step at around 80 m, which was reported to be related to a sea-level lowstand delta system (Urien and Ewing, 1974; Urien et al., 1995). Several canyons dissect the continental slope off northern Argentina and Uruguay. Some of these canyons cut back into the shelf break but do not show

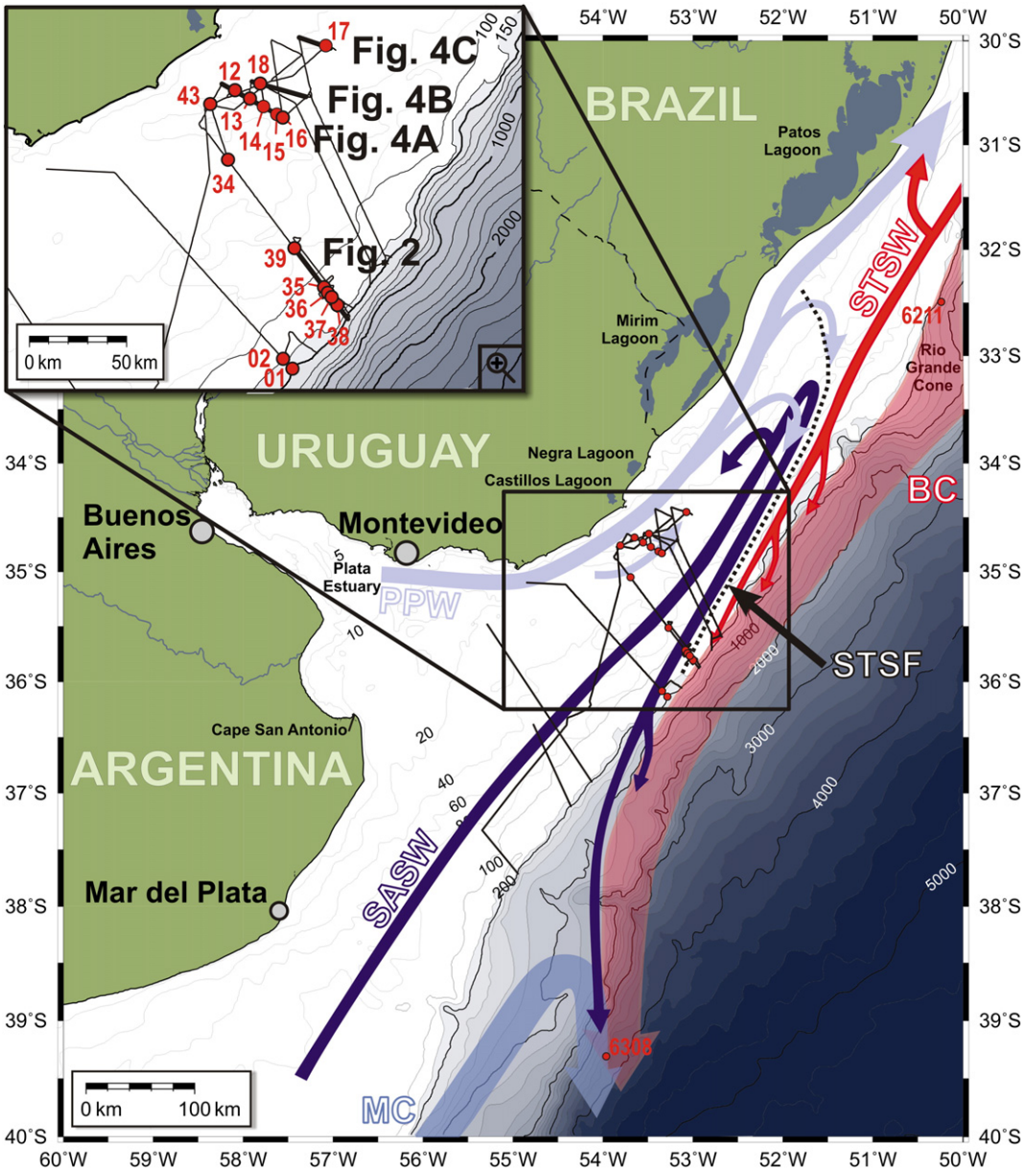

Figure 1. Map of the study area showing acoustic profiles, core positions, and oceanography (base map modified from Bender et al., 2013). Core positions of cruise M78/3 are displayed in short form (e.g., GeoB13817-2 is depicted as "17"). Core positions from cruises M46-2 and M46-3 are displayed as 4-digits (e.g., GeoB6211-2 is depicted as "6211"). Shelf water masses (PPW = Plata Plume Water; SASW = Subantarctic Shelf Water; STSW = Subtropical Shelf Water), their front (STSF = Subtropical Shelf Front), and currents at the continental slope (BC = Brazil Current; MC = Malvinas Current) are displayed as arrows based on Piola et al. (2008). Bathymetric data stems from Martins and Corrêa (1996) and GEBCO (2008). Inlay map shows a magnification of the Uruguayan shelf and location of the acoustic profiles displayed in Figs. 2 and 4 (thick black lines).

https://doi.org/10.1016/j.yqres.2014.01.003 Published online by Cambridge University Press

major incisions on the shelf itself (Lonardi and Ewing, 1971; Harris and Whiteway, 2011). Furthermore, the continental slope off northern Argentina displays several morphological terraces, such as Ewing Terrace and Necochea Terrace (Hernández-Molina et al., 2009; Preu et al., 2012, 2013). Farther north, the semicircular-shaped Rio Grande Cone off southern Brazil represents the most characteristic morphological feature (Fig. 1). It has been dominantly constructed from mudstones and shale since the Miocene (Fontana, 1996; Chiessi et al., 2008; Castillo et al., 2009).

Oceanography and sea-level history

The modern Plata Estuary discharges on average 23,000 $m^3\ s^{-1}$ of freshwater into the South Atlantic (Tossini, 1959). The resulting low-salinity tongue (Plata Plume Water [PPW]; Fig. 1) shows a strong displacement towards the northeast in austral winter due to predominately southwesterly winds. In austral summer, northeasterly winds force a southwestward retreat of the PPW, spreading low-salinity waters over the entire continental shelf off the Plata Estuary (Guerrero et al., 1997; Piola et al., 2000).

Two distinct water masses form the subsurface shelf hydrography: the northward-flowing cold and less saline Subantarctic Shelf Waters (SASW) and the southward-directed warm and salty Subtropical Shelf Waters (STSW; Piola et al., 2000; Fig. 1). The Subtropical Shelf Front (STSF) forms the sharp thermohaline boundary between SASW and STSW (Fig. 1). Subsurface water mass distribution and STSF location present only minor seasonal variability (Möller et al., 2008; Piola et al., 2008). The STSF is suggested to be the shelf-ward continuation of the Brazil–Malvinas Confluence Zone (BMC), which marks the boundary zone between the cold northward-flowing Malvinas Current (MC) and the warm southward-directed Brazil Current (BC; Piola et al., 2000; Fig. 1). At deeper water levels the northward-flowing Antarctic Intermediate Water (AAIW), Circumpolar Deep Water (CDW) and Antarctic Bottom Water (AABW) encounter a southward flowing recirculated branch of the AAIW and the North Atlantic Deep Water (NADW; Georgi, 1981; Saunders and King, 1995; Piola and Matano, 2001; Carter and Cortese, 2009). We refer to the modern terms of these water masses and currents when discussing their ancient equivalents although their properties (e.g., salinity, temperature, vertical stratification, and intensity) may have varied during the late Quaternary.

Reliable information on late Quaternary sea-level fluctuations in the region is scarce. Two relative sea-level curves were published by Guilderson et al. (2000) and Cavallotto et al. (2004), spanning the past 20 and 10 cal ka BP, respectively, with the latter curve calibrated by Gyllencreutz et al. (2010). According to Guilderson et al. (2000), a minimum sea level of −150 m was reached during the last glacial maximum (LGM). The maximum sea-level highstand of +6.5 m occurred at 6.5 cal ka BP (Gyllencreutz et al., 2010). Recently, Martínez and Rojas (2013) reviewed Holocene sea-level reconstructions in the Uruguayan region and showed that the sea level declined rather constantly since at least 6 cal ka BP.

Stratigraphic architecture

Only few studies provide data on the shelf stratigraphy of the study area. Ewing and Lonardi (1971) defined two nearly horizontal seismic reflectors on the shelf at 139–146 m and 200 m below modern sea level (mbsl). The deeper reflector was suggested to be associated to the Pliocene–Pleistocene boundary, whereas the shallower reflector might represent the base of fluvially derived deposits. Parker et al. (2008) defined six depositional sequences separated by strong seismic reflectors. The uppermost sequence represents the last post-glacial transgressive event. In addition, Martins et al. (2005) observed Cenozoic delta complexes at the shelf break. However, the seismic approach of these studies did not provide the necessary resolution for late Quaternary studies and led to an oversimplification of the shelf architecture.

The stratigraphy of the continental slope off northern Argentina gained more attention during the past years as part of one of the world's major contourite depositional system, recently mapped and classified by Hernández-Molina et al. (2009) and Preu et al. (2012, 2013). The complex terraced slope off northern Argentina evolved since middle to late Miocene (Hernández-Molina et al., 2009; Violante et al., 2010).

Sedimentary shelf system

In the modern system, two main sediment sources contribute material to the shelf of the study area: (1) the Plata drainage basin and (2) the Argentine margin (Mahiques et al., 2008). The Uruguay and Paraná Rivers discharge a suspended sediment load of 100 Mt yr^{-1} (Milliman and Farnsworth, 2011). Reconstructions of modern sediment discharge routes from the Plata Estuary onto the shelf were based on the surface sediment distribution. According to Martins and Corrêa (1996), the major part of the suspended sediment load is deflected sharply towards the north as soon as the plume enters the South Atlantic. There, the Plata paleo-valley represents the main modern sediment sink on the shelf for this clayey to silty material (Urien, 1972; Urien and Ewing, 1974; Ayup, 1987). Redeposited material from the Argentine margin was found to be transported at least up to 37°S under modern conditions (Mahiques et al., 2008).

In contrast to the modern sedimentary system, little is known on the past distribution of material as well as the age and location of depocenters. The main sediment pathways of the Plata during glacial stages were reconstructed by the pioneering studies of Lonardi and Ewing (1971), Urien and Ottmann (1971), Urien and Ewing (1974), and Urien et al. (1980a,b). However, the pathways are partly contrasting and suggested courses (1) towards the northern Argentine slope, (2) just to the east of the Plata Estuary, and (3) to the Uruguayan and SE Brazilian shelf. The pre-Holocene distribution of material from the Argentine margin has remained completely unclear up to now. This gap in knowledge, and the contradiction concerning possible transport pathways during periods of shelf exposure, underline the demand for a comprehensive study analyzing the fate of the large volumes of fluvial material supplied at particular time intervals, as well as clarifying the long-term sedimentary evolution of the margin off the Plata Estuary.

Materials and methods

Acoustic profiling and sediment coring

Sediment-acoustic data were collected by means of a PARASOUND P70 system during the Cruise M78-3 with the German research vessel METEOR (Krastel et al., 2012; Fig. 1). The primary high and low frequencies of the system were set to 18 and 22 kHz, respectively, leading to a secondary parametric signal of 4 kHz for sub-bottom profiling.

The 20 GeoB-cores of this study were collected during the M46-2, M46-3, and M78-3 cruises performed with the research vessel METEOR (Bleil et al., 2001; Schulz et al., 2001; Krastel et al., 2012; Fig. 1; Table 1). Vibrocorer and gravity corer were used to recover sandy and muddy sediments, respectively. In addition, a giant box corer was deployed to sample the undisturbed modern sediment surface (Table 1).

Laboratorial analyses

Detailed visual descriptions were performed for every sediment core. 200 representative samples were chosen for grain-size analysis to validate the visual core descriptions. The coarse fraction (>63 μm) was separated from the fine fraction (<63 μm) by wet sieving. Afterwards, the coarse fraction was sonic-sifted into subfractions. The scheme of Blair and McPherson (1999) was used to classify the sediments. Pictures of sediment cores were recorded by either standard digital camera or a color line scanner consisting of a GEOSCAN III camera with red, green and blue detectors (RGB).

https://doi.org/10.1016/j.yqres.2014.01.003 Published online by Cambridge University Press

Table 1
Location of sediment cores and surface samples investigated in this study.

Core position (GeoB)	Latitude (S)	Longitude (W)	Water depth [m]	Recovery [cm][a]	Coring device[b]
6211-2	32°30.31′S	50°14.56′W	657	774	GC
6308-3	39°18.10′S	53°57.90′W	3620	793	GC
13802-1	36°05.30′S	53°20.72′W	142.1	ss	GBC
13802-2	36°05.30′S	53°20.72′W	141.6	341	VC
13812-3	34°41.61′S	53°38.97′W	33.3	ss	GBC
13813-1	34°44.21′S	53°33.29′W	58	ss	GBC
13813-4	34°44.22′S	53°33.27′W	57.1	1028	GC
13814-1	34°46.68′S	53°28.11′W	40.1	ss	GBC
13814-2	34°46.68′S	53°28.10′W	39.3	64	GC
13814-3	34°46.68′S	53°28.19′W	39.5	504	VC
13815-1	34°49.04′S	53°23.08′W	47.3	ss	GBC
13815-2	34°49.05′S	53°23.10′W	46.6	506	VC
13816-3	34°50.04′S	53°20.92′W	44.5	ss	GBC
13816-4	34°50.06′S	53°20.93′W	44.5	506	VC
13817-2	34°27.55′S	53°04.52′W	61.9	1111	GC
13817-3	34°27.54′S	53°04.51′W	62.4	ss	GBC
13818-1	34°39.41′S	53°29.36′W	40.1	ss	GBC
13818-2	34°39.41′S	53°29.36′W	40.2	103	VC
13818-3	34°39.41′S	53°29.36′W	40.4	267	VC
13818-4	34°39.41′S	53°29.36′W	40.6	504	VC
13834-1	35°03.27′S	53°41.74′W	16.2	ss	GBC
13834-2	35°03.29′S	53°41.74′W	16.5	485	VC
13835-1	35°43.10′S	53°05.13′W	131	ss	GBC
13835-2	35°43.10′S	53°05.13′W	131.1	502	VC
13835-3	35°43.11′S	53°05.14′W	131	432	GC
13836-1	35°44.72′S	53°03.66′W	134.7	ss	GBC
13836-2	35°44.72′S	53°03.66′W	134.6	496	VC
13837-1	35°46.18′S	53°02.31′W	167.5	ss	GBC
13837-2	35°46.18′S	53°02.29′W	140.1	313	VC
13838-1	35°48.69′S	52°59.97′W	148.4	ss	GBC
13838-2	35°48.69′S	52°59.97′W	150.8	499	VC
13839-1	35°30.87′S	53°16.43′W	66.8	485	VC
13843-1	34°45.88′S	53°48.51′W	37.0	382	VC
13939-2	35°30.87′S	53°16.43′W	67.1	ss	GBC

[a] ss = surface sample.
[b] Coring device: GC = gravity corer; VC = vibrocorer; GBC = giant box corer.

Although Nd values can be grain-size dependent (e.g., Revel et al., 1996; Innocent et al., 2000), Goldstein et al. (1984) and Mahiques et al. (2008) demonstrated that grain size has no significant influence on the Nd signals along the E South American margin. Therefore, Neodymium (Nd) isotopic analysis was applied to the bulk lithological fraction of 42 samples (Table 2). However, since most of the samples of Mahiques et al. (2008) were composed of silts, our interpretations about the origin of sands are based on the assumption that Nd values do not differ between size fractions. Part of the samples were prepared and analyzed at the Earth Science Department, University of Bristol, following Vance and Thirlwall (2002) and Stoll et al. (2007), while the rest were prepared and analyzed at the Institute of Geosciences, University of São Paulo, following Sato et al. (1995). Sample treatment was similar in both laboratories and involves the removal of carbonate, digestion with HF–HNO_3, and elemental separation in HCl. Measurements were performed on a Thermo-Finnigan Neptune multicollector inductively coupled plasma mass spectrometer at the University of Bristol and on a Thermo-Scientific TRITON multicollector thermal ionization mass spectrometer. Nd data are presented in εNd units, the deviation of a sample $^{143}Nd/^{144}Nd$ from the present-day chondritic reservoir value (CHUR = 0.512638) in parts per 10,000.

Radiocarbon dating of 37 samples was carried out at the Poznań Radiocarbon Laboratory (Poland; Table 3). 14 ages were originally published by Chiessi et al. (2008) and Razik et al. (2013). Raw ^{14}C ages were converted into 1-sigma calibrated ages using the Calib 6.1.1 software and the Marine09 calibration data set, including a standard reservoir age of 405 years (Stuiver et al., 1998; Reimer et al., 2009). All ages are reported in calibrated thousands of years before present (cal ka BP).

Results

Shelf architecture and sedimentary characteristics of the stratigraphic units

Within the studied area, the shelf break occurs at water depths of 150 to 165 m (Figs. 1 and 2). The shelf shows a variable seafloor topography. Whereas the outermost shelf is characterized by a terrace-like shape and a smooth relief, the outer- to mid-shelf display a relatively rough surface (Fig. 2). Moreover, the inner-shelf features the SW–NE running morphological depression of the Plata paleo-valley, 40 km off the Uruguayan coast (Fig. 4). This depression was about 35 km wide and up to 50 m deep before it became partly filled by sediments. Its present-day seafloor physiography was described by Urien and Ottmann (1971), Urien and Ewing (1974), Urien et al. (1980a,b), and Cavallotto and Violante (2005).

PARASOUND profiling was used to define nine main units (U1–U9) on the shelf according to their bounding unconformities and their acoustic facies (Figs. 2–5). Sediment properties provided information on the depositional environments of the units. It has to be noted that additional local depocenters beyond the resolution of the presented dataset and erosion of former depocenters cannot be excluded.

U9 is the stratigraphically oldest unit. Its extent is restricted to the outer shelf. A maximum thickness of ~30 m is reached close to the shelf break with progradational acoustic geometries (Fig. 2). At their landward-directed limit, the internal reflections show aggradational patterns and toplap terminations. The sedimentary facies remains unclear due to the limited core penetration. U8 is also restricted to the outer shelf with a maximum thickness of 22 m close to the onlapping landward limit of this unit (Fig. 2). The thickness of U8 gradually

https://doi.org/10.1016/j.yqres.2014.01.003 Published online by Cambridge University Press

Table 2
Neodymium isotopic data. The age of the samples is calculated based on: (1) detailed age models of Cores GeoB6211-2 and GeoB6308-3 (Fig. 7); and (2) linear age models of Cores GeoB13814-3, GeoB13817-2, GeoB13834-2, and GeoB13835-2. Age estimations of Cores GeoB13802-2, GeoB13836-2, GeoB13838-2, and GeoB13839-1 are based on single radiocarbon dates in combination with the sea level curve of Guilderson et al. (2000).

Core no. (GeoB)	Depth in core (cm)	143Nd/144Nd	2σ	εNd	Age (cal ka BP)	Strat. unit
6211-2	1	0.512175	0.000008	−9.02	0	RGC
6211-2	5	0.512185	0.000008	−8.84	0.3	RGC
6211-2	10	0.512189	0.000011	−8.77	0.7	RGC
6211-2	20	0.512222	0.000010	−8.12	1.5	RGC
6211-2	25	0.512233	0.000006	−7.90	2.0	RGC
6211-2	35	0.512255	0.000007	−7.47	3.0	RGC
6211-2	45	0.512246	0.000010	−7.64	3.9	RGC
6211-2	55	0.512279	0.000011	−7.00	4.9	RGC
6211-2	65	0.512277	0.000010	−7.04	6.4	RGC
6211-2	70	0.512257	0.000009	−7.43	7.2	RGC
6211-2	82	0.512133	0.000007	−9.86	9.4	RGC
6211-2	90	0.512115	0.000011	−10.21	10.4	RGC
6211-2	95	0.512133	0.000006	−9.85	10.6	RGC
6211-2	110	0.512120	0.000006	−10.10	12.4	RGC
6211-2	120	0.512133	0.000008	−9.85	13.7	RGC
6211-2	180	0.512116	0.000009	−10.17	14.9	RGC
6211-2	280	0.512150	0.000008	−9.53	16.4	RGC
6211-2	380	0.512148	0.000007	−9.57	17.8	RGC
6211-2	480	0.512142	0.000011	−9.67	18.4	RGC
6211-2	579	0.512149	0.000009	−9.54	19.1	RGC
6308-3	8	0.512421	0.000012	−4.23	1.5	NTD
6308-3	53	0.512432	0.000010	−4.03	5.7	NTD
6308-3	135	0.512480	0.000013	−3.09	12.8	NTD
6308-3	247	0.512498	0.000015	−2.70	19.2	NTD
6308-3	336	0.512466	0.000012	−3.35	23.3	NTD
6308-3	473	0.512483	0.000008	−3.03	29.5	NTD
6308-3	588	0.512472	0.000007	−3.20	40.6	NTD
6308-3	616	0.512493	0.000010	−2.82	43.5	NTD
6308-3	675	0.512492	0.000008	−2.80	47.9	NTD
6308-3	750	0.512513	0.000012	−2.40	52.9	NTD
13802-2	202	0.512612	0.000003	−0.49	~16.5	U6
13814-3	298	0.512301	0.000004	−6.58	2.0	U2
13817-2	175	0.512109	0.000003	−10.32	0.3	U1
13817-2	775	0.512198	0.000002	−8.58	12.6	U3
13834-2	303	0.512359	0.000005	−5.45	1.9	U2
13835-2	48	0.512609	0.000003	−0.56	1.3	U5
13835-2	298	0.512617	0.000003	−0.41	8.2	U5
13836-2	348	0.512568	0.000003	−1.37	~15.5	U6
13838-2	73	0.512613	0.000005	−0.49	~19	U6
13838-2	305	0.512114	0.000003	−10.23	~45	U8
13839-1	112	0.512590	0.000003	−0.94	~11	U6
13839-1	464	0.512507	0.000004	−2.55	~45	U7

decreases towards the southwest where this unit vanishes. The general acoustic patterns of U8 show aggradation and erosional truncation of the top. Progradation at the shelf break is less developed than in U9 (Fig. 2). Retrieved sediments consist of stiff gray mud, partly enriched in mollusc shells and shell fragments (Figs. 3 and 6). The progradational U7 downlaps onto U8 and older strata, and shows oblique reflection pattern (Fig. 2). This unit extends from the mid-shelf (~25 m water depth) towards the outer shelf down to a maximum water depth of ~125 m, where it truncated into U8. Maximum thickness of U7 is 11 m and the deposits consist of greenish gray to grayish brown muddy fine sands to fine-sandy mud (Figs. 3 and 6). U6 overlies the erosional surface on top of U8 and U7. Although U6 covers large areas on mid- to outer shelf, it consists of laterally discontinuous sediment bodies with a common thickness of less than 5 m (Fig. 2). U6 shows only few internal reflectors with no systematic orientation. Dark gray fine sands and gravel composed of mollusc shells and shell fragments represent the dominating sediment types of U6 (Figs. 3 and 6). Aggradational U5 fills depressions between the sand bodies of U6 and covers the outer-shelf relief (Fig. 2). A maximum thickness of 10 m is reached on the outer shelf where the top of underlying U8 shows patterns of erosional truncation. U5 consists of olive gray muddy very fine sands (Figs. 3 and 6).

The distribution of U4 to U1 is almost entirely restricted to the SW–NE running Plata paleo-valley on the inner shelf off Uruguay (Fig. 4). Within this depression, U4 truncates into older strata. This unit shows a maximum thickness of 16 m but its distribution is very irregular, filling a complex pattern of steeply inclined incisions (Fig. 4). U3 shows aggradational internal acoustic reflection patterns (Fig. 4). The maximum thickness amounts to 28 m and the sedimentary facies types are highly differentiated. A sediment core from the central axis of the Plata paleo-valley (13817-2; Figs. 5 and 6) shows rhythmic mud lamination, intercalations of fine sands with abundant cross bedding, and small-scale erosive channels. In contrast, deposits from a marginal position within the paleo-valley range from pure mud to mollusc-fragment gravel (13818-4; Fig. 5). An erosional surface separates U3 and U2. Acoustic patterns of U2 are mainly semi-transparent but some distinctive sigmoid progradational reflections are present (Fig. 4). This unit forms a local sediment body with a maximum thickness of 14 m (Fig. 4). Sediments of U2 consist of homogenous very fine sands (Figs. 5 and 6). The boundary between U2 and U1 shows transitional characteristics (Fig. 4). U1 shows aggradational patterns in most parts along the valley but progradational internal stratification also occurs. The maximum thickness of U1 is 12 m and the sediments predominantly consist of very fine silt (Figs. 5 and 6).

Two additional sediment cores from the adjacent continental slope are used to investigate sediment transport directions and off-shelf export patterns. Core 6211-2 is located at the Rio Grande Cone off Southern Brazil (Fig. 1). The acoustic profile displays a well-stratified

https://doi.org/10.1016/j.yqres.2014.01.003 Published online by Cambridge University Press

Table 3
Accelerator mass spectrometry (AMS) radiocarbon dates and calibrated ages.

Lab No.[a]	Core no. (GeoB)	Depth in core (cm)	Material[b]	Age (^{14}C yr BP)	Age (cal yr BP, 1σ)[c]	Strat. unit	Reference
–	6211-2	1	–	–	modern[d]	RGC	
KIA30528	6211-2	18	pF	1685 ± 30	1281–1217	RGC	Chiessi et al. (2008)
KIA35166	6211-2	35	pF	3170 ± 40	3030–2893	RGC	Razik et al. (2013)
KIA35165	6211-2	55	pF	4625 ± 45	4900–4799	RGC	Razik et al. (2013)
KIA30527	6211-2	73	pF	7145 ± 55	7662–7565	RGC	Chiessi et al. (2008)
NOSAMS75186	6211-2	86	pF	9370 ± 40	10,240–10,170	RGC	Razik et al. (2013)
KIA35163	6211-2	95	pF	9920 ± 70	11,020–10,730	RGC	Razik et al. (2013)
–	6211-2	98	–	–	10,790[e]	RGC	
KIA35162	6211-2	101	pF	9810 ± 110	10,825–10,556	RGC	Razik et al. (2013)
KIA30526	6211-2	123	pF	12,600 ± 70	14,148–13,934	RGC	Chiessi et al. (2008)
KIA30525	6211-2	218	pF	13,340 ± 80	15,656–15,144	RGC	Chiessi et al. (2008)
KIA30524	6211-2	358	pF	14,860 ± 90	17,836–17,429	RGC	Chiessi et al. (2008)
KIA30531	6211-2	448	bv	15,590 ± 100	18,288–18,114	RGC	Chiessi et al. (2008)
KIA30530	6211-2	583	bv	16,400 ± 120	19,316–18,982	RGC	Chiessi et al. (2008)
Poz-43433	6308-3	4	pF	1500 ± 30	1094–992	NTD	
Poz-43435	6308-3	16	pF	2770 ± 30	2583–2423	NTD	
Poz-43436	6308-3	28	pF	3645 ± 30	3595–3490	NTD	
Poz-43437	6308-3	40.5	pF	4490 ± 35	4775–4635	NTD	
Poz-43438	6308-3	52	pF	5240 ± 25	5625–5574	NTD	
Poz-43439	6308-3	64	pF	6290 ± 40	6794–6680	NTD	
Poz-43440	6308-3	76	pF	7310 ± 40	7825–7718	NTD	
Poz-43441	6308-3	88	pF	8970 ± 40	96,74–9546	NTD	
Poz-43442	6308-3	100	pF	9930 ± 50	10,947–10,758	NTD	
Poz-43443	6308-3	107	pF	10,130 ± 50	11,187–11,117	NTD	
–	–	242	–	–	19,000[f]	NTD	
–	–	484	–	–	30,000[f]	NTD	
–	–	631	–	–	45,000[f]	NTD	
–	–	767	–	–	54,000[f]	NTD	
Poz-36091	13802-2	340 (base)	bv (D)	14,200 ± 70	16,981–16,801	U6	
Poz-36092	13802-2	340 (base)	bv (V)	14,060 ± 60	16,892–16,718	U6	
Poz-42431	13813-4	964	bv piece	1600 ± 30	1220–1125	U1	
Poz-36085	13814-3	491	bv	3455 ± 35	3384–3292	U2	
Poz-36086	13815-2	371	bv	3095 ± 35	2920–2810	U2	
Poz-36061	13815-2	500–502	bv, bF, os	9100 ± 50	9931–9714	U3	
Poz-42432	13817-2	538	bv	1385 ± 30	962–898	U1	
Poz-42433	13817-2	668.5	bv pieces	10,740 ± 110	12,347–11,948	U3	
Poz-42434	13817-2	996	plant debris	11,760 ± 70	13,710–13,498	U3	
Poz-36087	13818-4	208	bv	9740 ± 50	10,642–10,538	U3	
Poz-36088	13834-2	230	bv, co, bF, gp	1900 ± 30	1492–1400	U2	
Poz-36103	13835-2	479	bv	11,650 ± 60	13,235–13,096	U5	
Poz-36089	13838-2	177–179	bv, bF	16,680 ± 80	19,559–19,381	U6	
Poz-36104	13838-2	496–498	bF, os	43,500 ± 1800	48,197–44,909	U8	
Poz-36090	13839-1	429–431	bv, gp	10,020 ± 50	11,121–10,935	U6	

[a] Radiocarbon laboratory: KIA = Leibniz Laboratory in Kiel (Germany); NOSAMS = National Ocean Sciences Accelerator Mass Spectrometry Facility, Woods Hole Oceanographic Institution (USA); Poz = Poznań Radiocarbon Laboratory (Poland).
[b] Material: pF = planktonic foraminifers; bF = benthic foraminifers; bv = bivalves; gp = gastropods; co = coral pieces; os = ostracods.
[c] For reservoir correction, the conventional age of 405 years is applied using CALIB 6.1.1. (Reimer et al., 2009; Stuiver et al., 1998).
[d] The extrapolation of the calibrated 14C ages at 18 and 35 cm core depth results in an age close to 0 cal yr BP for the core top and allows assigning a modern age to the uppermost centimeters of the core sequence.
[e] Interpolated value between the ^{14}C ages at 95 and 101 cm depth.
[f] Because of the lack of carbonate, the age model for GeoB6308-3 below 107 cm core depth was established based on stratigraphic correlation of the 7th degree polynomial fit of GeoB6308-3 Fe/K record to February insolation at 30°S (Laskar et al., 2004).

deposit with aggradational acoustic patterns. Sediments consist of dark greenish gray clayey nannofossil ooze (Wefer et al., 2001). Core 6308-3 was retrieved from the central area of a contourite drift on the Necochea Terrace in ~3500 m water depth off northern Argentina (Hernández-Molina et al., 2009; Preu et al., 2013). Sediments are made up of dark gray muddy diatom ooze (Bleil et al., 2001). Hence, we define two sedimentary units for the continental slope based on the location of the respective cores: (1) a unit representing deposition at the Rio Grande Cone during the past sea-level cycle (RGC; Core 6211-2) and (2) a unit marking the Necochea Terrace Drift (NTD; Core 6308-3).

Age control

On the continental shelf, radiocarbon dating was applied to sediments of 6 units (Table 3). The formation times of U4, U7, and U9 remain unclear due to the limited coring depth or absence of fresh carbonate material and their ages are deduced from the stratigraphic context. A date of 48.2–44.9 cal ka BP in U8 (Core 13838-2; Fig. 3) links the formation of this unit to Marine Isotope Stage 3 (MIS 3). U7 prograded across the erosional surface on top of U8 (Fig. 2). The oldest date on U6 displays an age of 19.6–19.4 cal ka BP (13838-2; 151 m water depth; Fig. 3) and shows an initial deposition of U6 when sea level was at its lowest position during the last glacial maximum (LGM; Hanebuth et al., 2009). Cores 13802-2 (142 m water depth) and 13839-1 (67 m water depth) reveal U6 ages of 17.0–16.7 and 11.1–10.9 cal ka BP, respectively (Table 3). Hence, these younger ages occurring in shallower water depths indicate a transgressive development of this unit during deglacial sea-level rise. Contemporaneously to the later formation of U6 in shallower waters, the development of U5 took place in deeper waters of the outer shelf, which is shown by an age of 13.2–13.1 cal ka BP close to the base of Core 13835-2 (Figs. 2 and 3). The work of Bender et al. (2013) on an uppermost slope terrace within the study area indicates that the deposition of U5 is still active today. Hence, assuming a modern age of the core top and a linear sedimentation rate, the basal age of U5 at site 13835-2 would be ~16.5 cal ka BP.

https://doi.org/10.1016/j.yqres.2014.01.003 Published online by Cambridge University Press

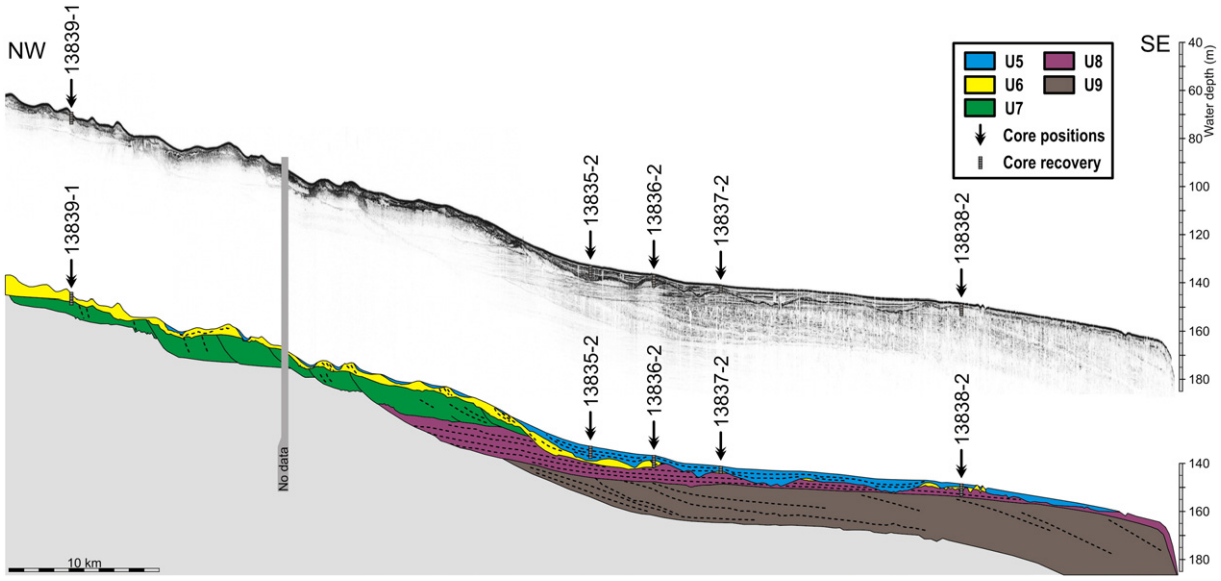

Figure 2. PARASOUND acoustic profile of the outer shelf (see Fig. 1 for location) and interpreted shelf architecture (vertical exaggeration = 160). U9–U5: main stratigraphic units. Black arrows indicate GeoB-core positions (see Fig. 3 for respective sediment core columns). Depth on y-axis is given in meters below modern sea level (mbsl).

The stratigraphic units on the inner shelf show generally younger depositional ages. Four radiocarbon dates on U3 range from 13.7 to 9.7 cal ka BP (Cores 13815-2, 13817-2, and 13818-4) and indicate formation during deglacial sea-level rise (Table 3). Two radiocarbon dates on the sandy U2 show ages of 3.4–3.3 (13814-3) and 2.9–2.8 cal ka BP (13815-2; Fig. 5). A date on this unit from the shelf plain adjacent to the Plata paleo-valley reveals a much younger age of 1.5–1.4 cal ka BP (13834-2; Table 3). The base of the U1 depocenter dates at 1.2–1.1 cal ka BP (13813-4; 964 cm) and 1.0–0.9 cal ka BP (13817-2; Fig. 5). Thus, extremely high sedimentation rates of 824 cm ka^{-1} (13813-4) and 598 cm ka^{-1} (13817-2) characterize U1. Interpolated maximum U1 basal ages of ~1.5 cal ka BP (13813-4) and ~1.2 cal ka BP (13817-2) display the initial onset of this depocenter at the respective positions. Presuming that the gradual change from sandy U2 to muddy U1 within the Plata paleo-valley took place at ~1.5 cal ka BP, U2 might have started to form around 4.6 cal ka BP (using a linear sedimentation rate of 270 cm ka^{-1} and a depocenter thickness of 12.5 m).

Sediments retrieved from the continental slope cover the past 54 cal ka BP (NTD) and 19 cal ka BP (RGC; Fig. 7). Both RGC and NTD are characterized by continuous sedimentation but sedimentation rates show a strong decrease during deglacial times (Fig. 7).

Provenance analysis

Lowest εNd values from the shelf are displayed by U8, U3, and U1 (−10.23, −8.58, and −10.32, respectively; Fig. 8). In contrast, all other units on the shelf exhibit considerably higher values. Four εNd values on U6 range between −0.49 and −1.37. U5 displays even higher measurements (−0.41 to −0.56), whereas U7 shows a value of −2.55. The exception to these cases represents U2, which displays intermediate values between −5.45 and −6.57. εNd values of RGC range from −7.00 to −10.21 and display, therefore, lower values than NTD (i.e. −2.4 to −4.23; Table 2).

Mahiques et al. (2008) subdivided two principle sources for surface sediments deposited off SE South America based on εNd measurements. The Plata province shows an average εNd value of −9.6. Sediments discharged from S Brazil display a comparable mean value of −9.3 and are, therefore, undistinguishable from the Plata province. In contrast, the Argentine margin province displays a much higher mean value of −1.9.

εNd measurements on sediments of the investigated stratigraphic units allow distinguishing between these two distinct sediment sources. Hence, U1, U3, and U8 plot in the field of the Plata province, U5, U6, and U7 belong to the Argentine margin province, and U2 represents a mixture of the two provinces (Fig. 8). The depocenters at the continental slope comprise longer time spans and show higher variability in their εNd signature. From 19 to ~9.5 cal ka BP, samples from RGC plot very consistently in the Plata Estuary field but show a marked shift towards higher values (mixed signature) between ~9.5 and ~5 cal ka BP (Fig. 8). After ~5 cal ka BP, a gradual decrease of εNd values occurs. Pre-Holocene samples from the NTD plot in the Argentine margin field but their assignment to this field is less pronounced than those of U6 and U5 (Fig. 8). Hence, pre-Holocene NTD samples show a tendency towards a mixed signal, which becomes more evident during and after deglacial sea-level rise.

The subdivision into two general sediment sources is well corroborated by the dominant grain-size fraction of the respective units. Samples with a Plata province εNd signature are characterized by muddy sediments, whereas material derived from the Argentine margin province predominantly displays very fine to fine sands.

Discussion

Facies interpretation of the units (depositional environments)

Two sites of this study are located at the continental slope. NTD represents a contourite drift formed on the Necochea Terrace on the lower slope (Preu et al., 2013). The sediment core within RGC stems from the upper slope. The well-stratified aggradational acoustic patterns and the predominance of clayey nannofossil ooze at this site indicate a depositional milieu, which was characterized by the settling of biogenic particles and of terrigenous fines from the Plata province (Fig. 8).

The progradational character of U9 and its location on the outermost shelf suggest a development during lower sea levels, possibly in form of a lowstand delta at the shelf edge as proposed by Urien and Ewing (1974) and Urien et al. (1980a, b). Precise age determination and facies classification would require sediment recovery from this unit.

U8 formed during MIS 3 (Table 3) and the material stemmed from the Plata province (Fig. 8). The widespread distribution and aggradational acoustic patterns of U8 argue against a proximal point source and delta-like progradation of the shelf. Instead, lateral advective

https://doi.org/10.1016/j.yqres.2014.01.003 Published online by Cambridge University Press

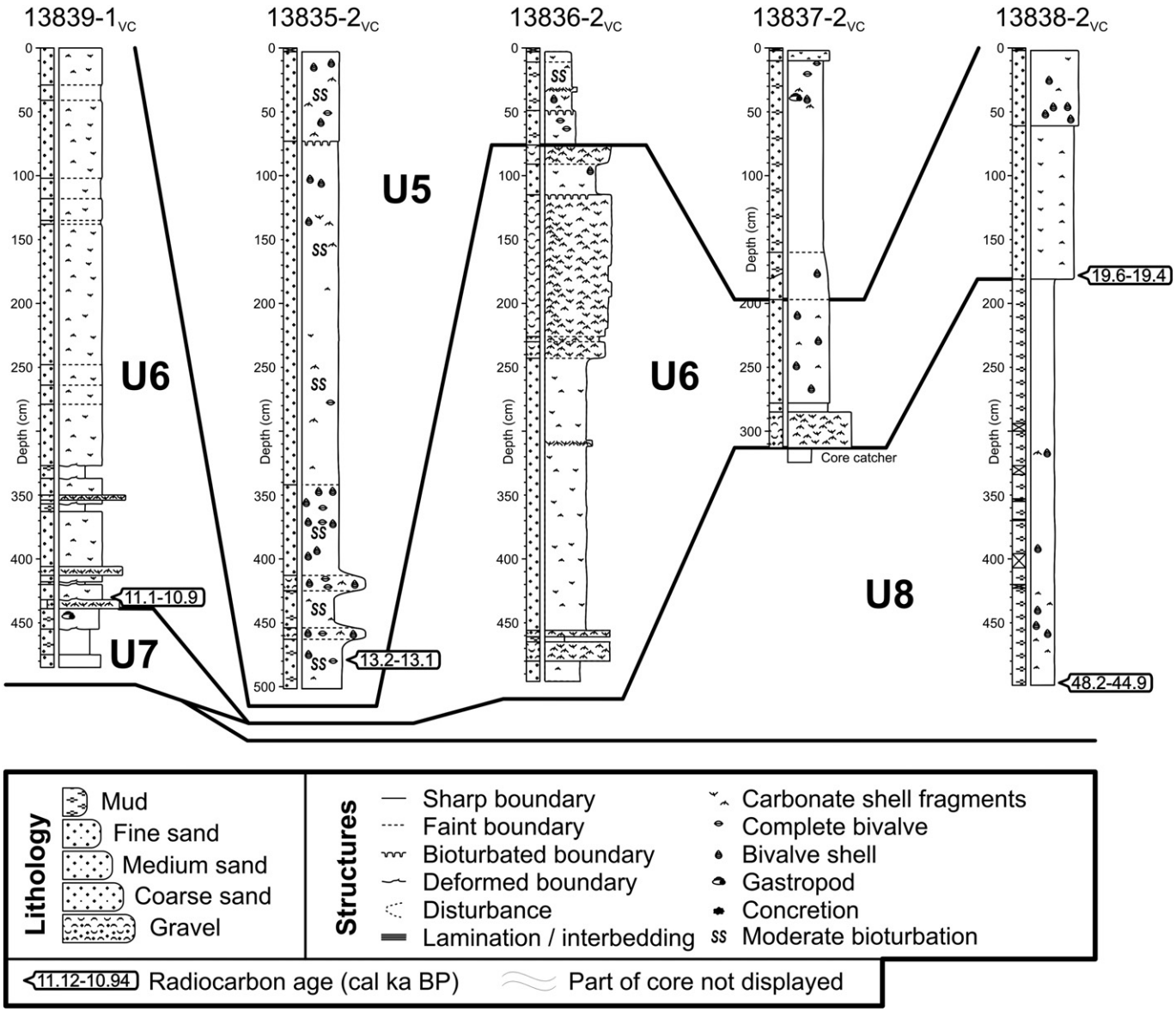

Figure 3. Sediment columns of GeoB-cores from the outer shelf (see Figs. 1 and 2 for location) displaying lithology, grain size and radiocarbon ages. Interpretation of acoustic profiles, core lithology and radiocarbon measurements enables the correlation of the stratigraphic units U8 to U5 between single cores.

transport by shelf currents represented the most likely mechanism of transporting mud to the location of U8. The dominantly fine-grained nature of U8 sediments points towards formation as a shelf mud depocenter below the storm wave base.

While the deposition of NTD, RGC, and U8 was restricted to deeper waters of the outer continental shelf and slope, U7 started to form during sea-level fall in mid-shelf position and downstepped towards the outer shelf where it truncated into U8 (Fig. 2). Also, U7 contains much higher sand content compared to U8 and shows a clear progradational trend. According to the nomenclature of Catuneanu et al. (2011), U7 is a typical deposit of a falling-stage systems tract. Hence, the material became deposited close to the shoreline and the material origin is closely linked to coastal processes such as erosion and longshore transport. Initial deposition of the transgressive U6 appeared already during LGM in a water depth of ~150 m (Figs. 2 and 3). A wide range in grain size (fine sands to gravel) and strong variations in thickness point towards the strong hydrodynamic conditions of shoreface environments. U6 deposits are very variable in shape and laterally discontinuous, which indicates that most of these drowned sediment bodies represent very local remnants of sea-level rise. Therefore, coastal processes dominated the formation of U6. The deposition of U6 at the shoreface is corroborated by a relative sea-level position of ~150 m during LGM based on the presence of shallow-neritic shell deposits on the outer shelf, which was proposed by Guilderson et al. (2000). On the outer shelf, the formation of U5 started at ~16.5 cal ka BP within depressions between the positive morphological features of U6 (Fig. 2). During further sea-level rise, these depositional patterns changed towards a drape-like appearance. The deposition in deeper waters compared to U6 indicates that these muddy very fine sands were directly controlled by the strength of the shelf current system rather than processes at the shoreface, as was the case for U6.

U4, U3, U2, and U1 are mainly restricted to the described inner-shelf depression (Fig. 4). Although the age of U4 remains unclear due to the limited coring depth, the acoustic facies indicates incised valley fills within the larger structure of the depression. Therefore, these channels became filled during sea-level rise and preceded the formation of U3. Major shelf accumulations of Plata-derived fines during deglacial sea-level rise are represented by U3 (Fig. 8). The sedimentary characteristics of U3 (i.e., lenticular bedding, rhythmic couplets of laminated mud and cross-bedded fine sands, erosive scours; Fig. 6) indicate a tidal origin.

https://doi.org/10.1016/j.yqres.2014.01.003 Published online by Cambridge University Press

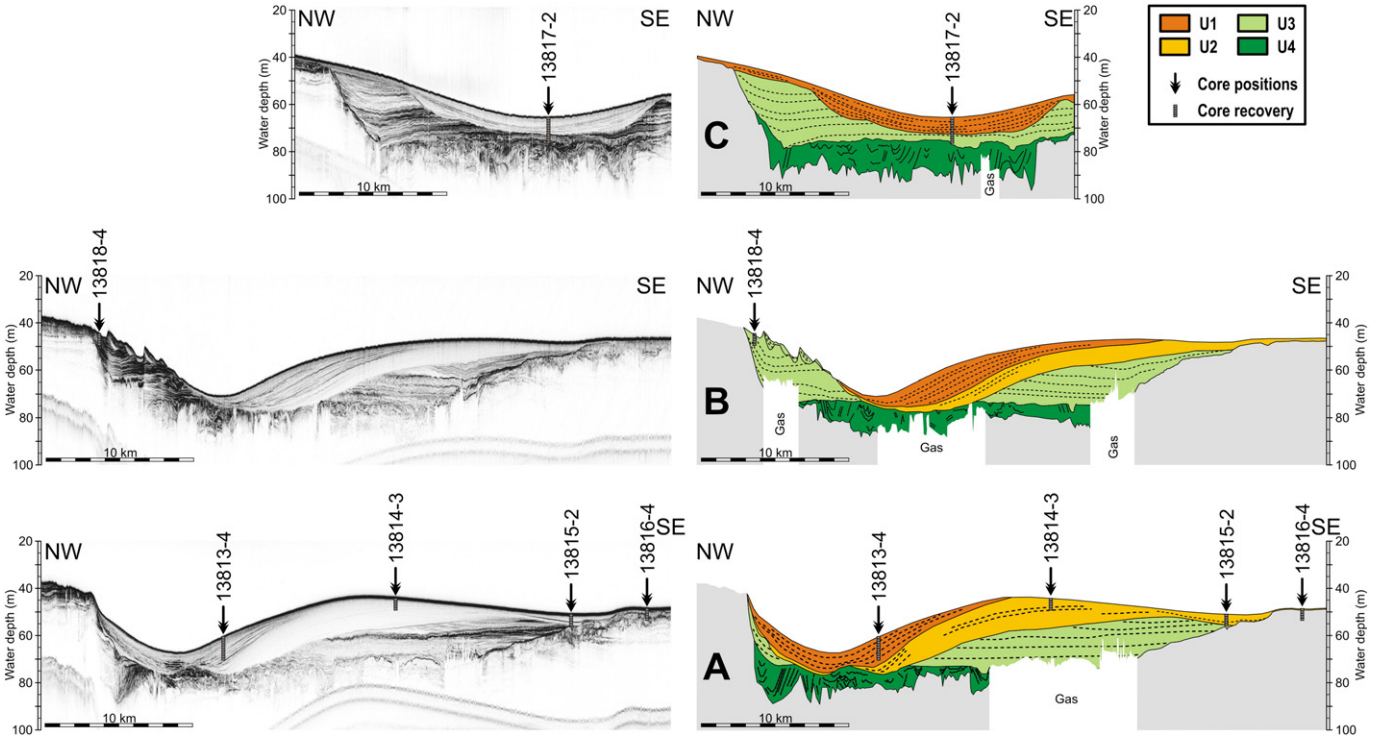

Figure 4. PARASOUND acoustic profiles of the inner shelf (see Fig. 1 for location) and interpreted shelf architecture (vertical exaggeration = 160). U4–U1: main stratigraphic units. Black arrows indicate GeoB-core positions (see Fig. 3 for respective sediment core columns). Depth on y-axis is given in meters below modern sea level (mbsl).

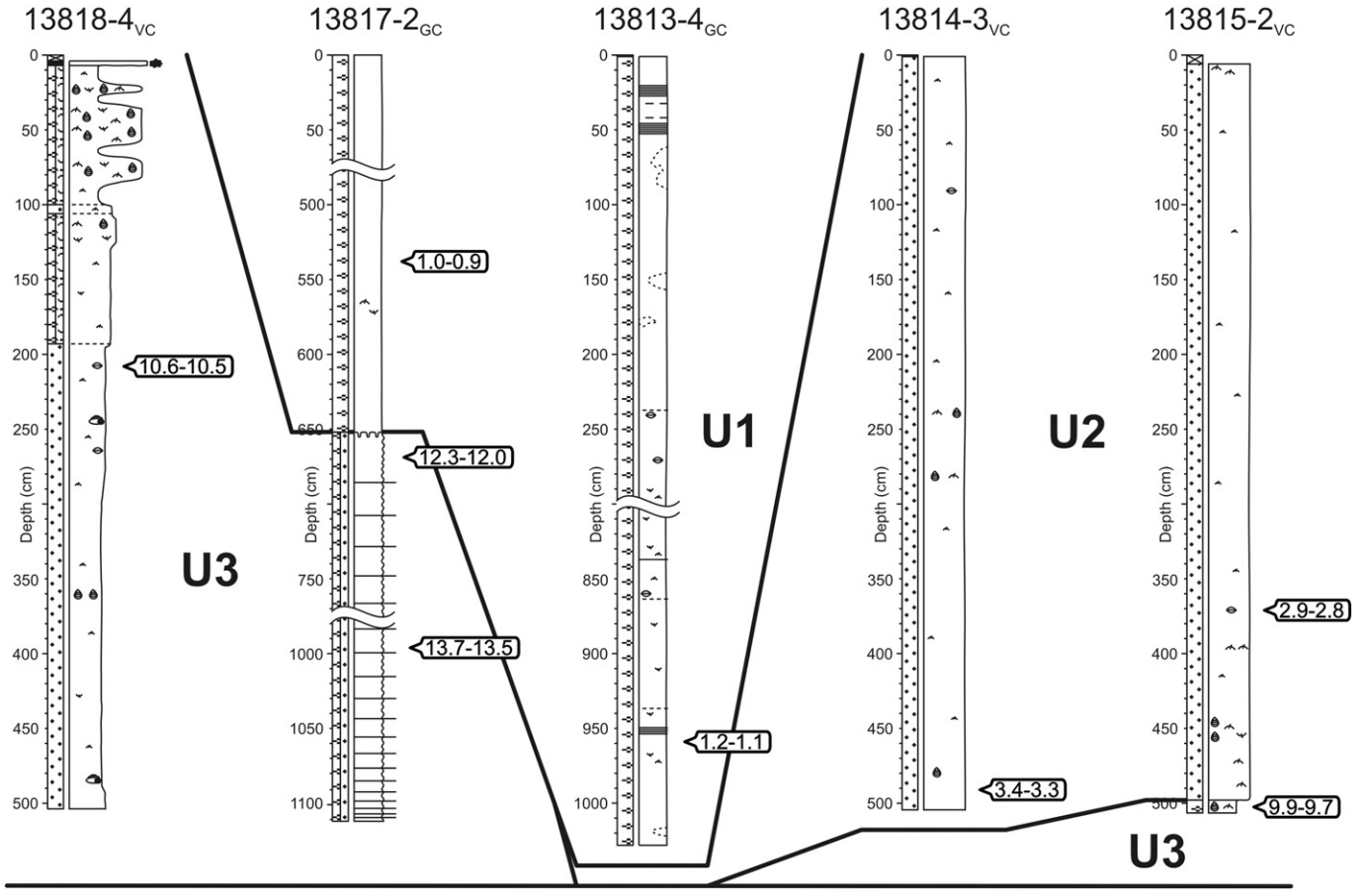

Figure 5. Sediment columns of GeoB-cores from the inner shelf (see Figs. 1 and 4 for location and Fig. 3 for legend) displaying lithology, grain size and radiocarbon ages. Interpretation of acoustic profiles, core lithology and radiocarbon measurements enables the correlation of the stratigraphic units U3 to U1 between single cores. For presentation reasons, parts of the columns of Cores GeoB13813-4 and GeoB13817-2 are cut out due to their homogenous lithology. Intercalated sand layers of Core GeoB13817-2 are displayed in a schematic way (see Fig. 6 for a detailed view on the lithology of this sediment core).

https://doi.org/10.1016/j.yqres.2014.01.003 Published online by Cambridge University Press

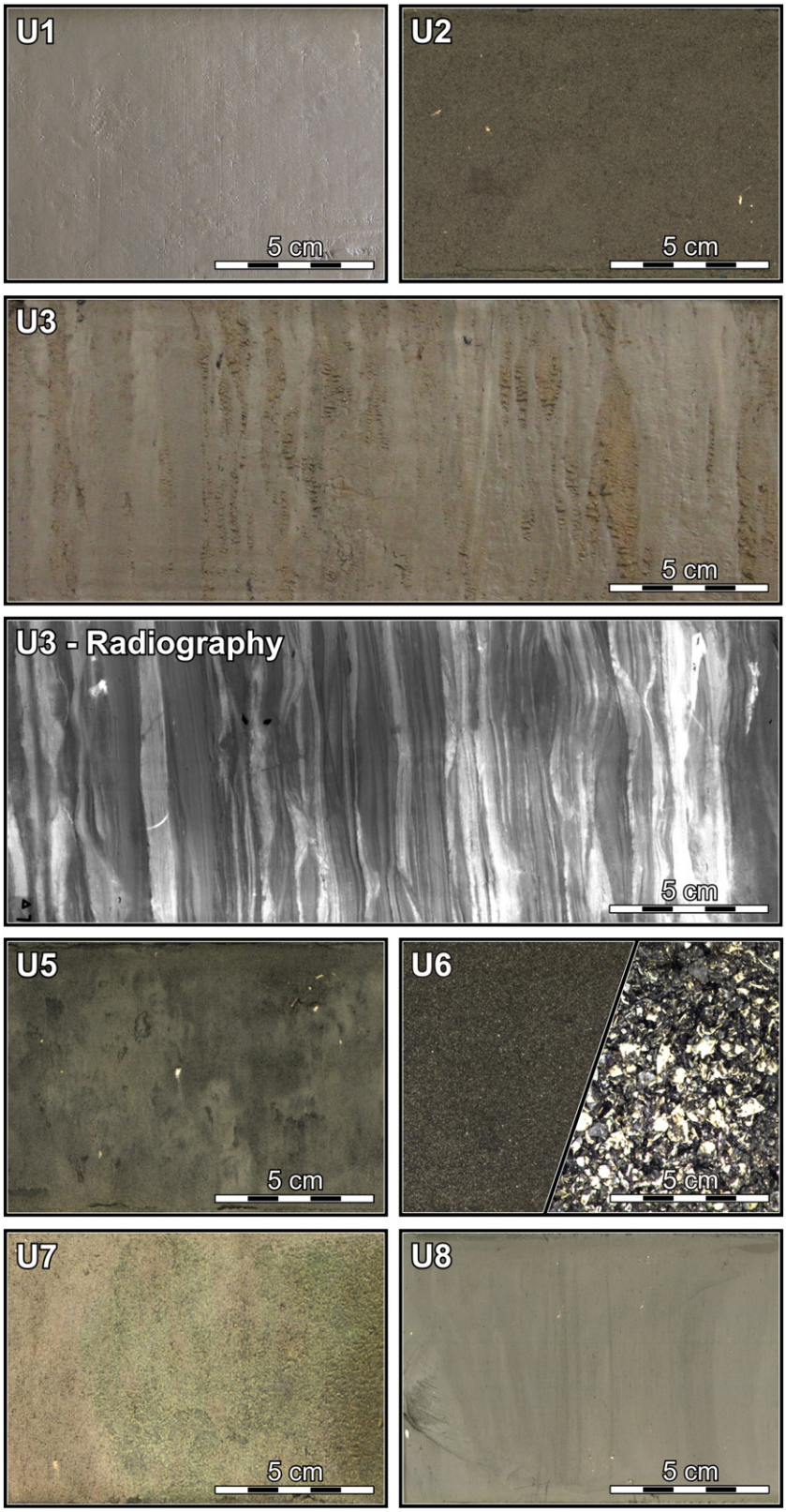

Figure 6. Core pictures, RGB color line scans, and a radiography showing the sedimentary characteristics of the main stratigraphic units. Displayed core sections, material, and type of image: (U1) Core GeoB13817-2, 102–114 cm; mud; photo; (U2) GeoB13814-3, 362–374 cm; slightly muddy very fine sand; RGB color line scan; (U3) GeoB13817-2, 992–1017 cm; intercalation of mud and fine sands; photo and radiography (denser material displayed in darker tones of gray); (U5) GeoB13835-2, 224–236 cm; muddy very fine sand; RGB color line scan; (U6) GeoB13836-2, 439–450 cm; very fine to fine sand; RGB color line scan; (U7) GeoB13839-1, 472–484 cm; muddy fine sand; RGB color line scan; (U8) GeoB13838-2, 372–384 cm; mud; RGB color line scan.

https://doi.org/10.1016/j.yqres.2014.01.003 Published online by Cambridge University Press

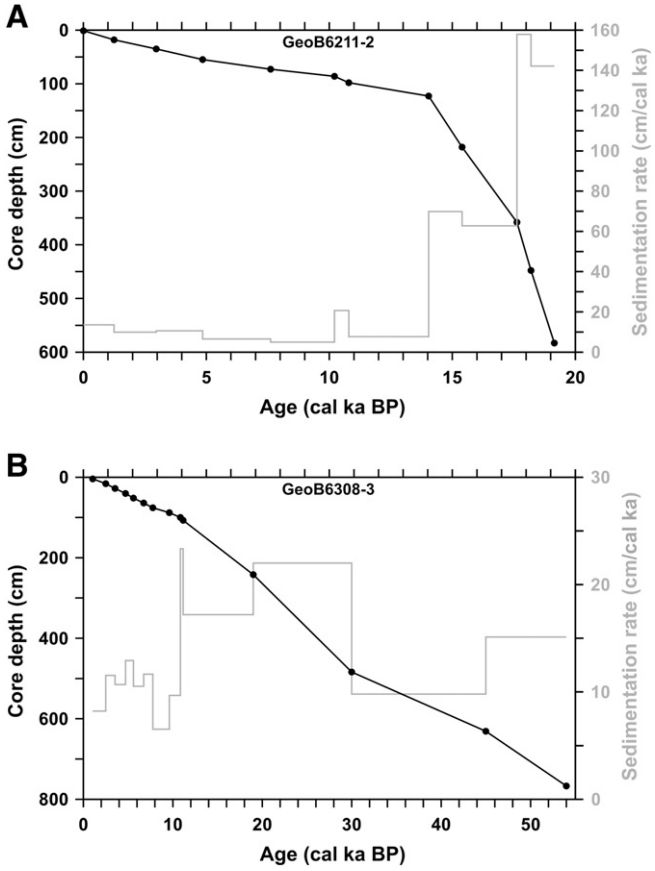

Figure 7. Age models and sedimentation rates of the two GeoB-cores retrieved from the continental slope; (A) Core GeoB6211-2; RGC; (B) Core GeoB6308-3; NTD (see Fig. 1 for locations).

The restriction to the shelf depression implies estuarine conditions during the deglacial flooding of this feature.

U2 represents a local inner-shelf sand depocenter mostly confined to the observed depression. The initial emplacement of U2 appeared at ~4.6 cal ka BP when sea level was approximately 2.5 m higher than today (Martínez and Rojas, 2013). Therefore, this unit developed under fully marine conditions. U2 represents a mixture of material derived from Argentine margin and Plata province (Fig. 8). The progradation of this sediment body towards the NW implies a transport by shelf currents from a southern region, namely the Argentine margin. The contribution of Plata fines appeared most probably by settling from the suspension plume of this estuary. In contrast, U1 sediments show a clear Plata province signature (Fig. 8). Mud accumulations of U1 started at around 1.5 cal ka BP. Hence, U1 represents a relatively modern shelf mud depocenter within the observed inner-shelf depression.

The course of the Plata River since the LGM

The specific location of the Plata paleo-valley played an important role for the sediment distribution during stages of lower sea level and is a prerequisite to study late Quaternary depocenter shifts. Our acoustic profiles suggest that the paleo-valley represents the only major fluvial incision on the shelf of the study area. The examination of sediment sources should provide additional information on the specific course of the Plata sedimentary pathway. Provenance of continental slope sediments in this study reveals: (1) a predominant contribution of material from the Argentine margin towards the continental slope off northern Argentina during the last sea-level cycle (NTD, Fig. 8); and (2) persistent supply of Plata sediments to the Rio Grande Cone at least since the LGM (RGC, Fig. 8). Furthermore, the Plata provenance of U3 and its deglacial age display that sediments from the Plata drainage basin filled the inner-shelf depression off Uruguay during deglacial sea-level rise (Figs. 4, 5, and 8). Hence, our data reveal that this major depression was the sole transport pathway for fluvial material from the Plata province during the past sea-level cycle, representing the paleo-valley of this river. Former reconstructions of the Plata drainage pathway on the exposed shelf during the LGM (Lonardi and Ewing, 1971; Urien and Ottmann, 1971; Urien and Ewing, 1974; Urien et al., 1980a,b) proposed (1) widespread branched incisions and an extensive lowstand delta at the shelf edge; (2) an abrupt northeastward inflection of the Plata paleo-valley at the exit of the estuary and further transport of the material towards Uruguayan continental slope and the Rio Grande Cone; and (3) numerous lowstand deltas on the outer northern Argentine and Uruguayan shelf, and deposition within the Rio Grande Cone as a result of several respective sediment pathways. Neither another major shelf incision nor LGM lowstand deltas are present in our acoustic profiles. Moreover, the high elevation difference between the wide coastal hinterland and the exposed outer-shelf plain during sea-level lowstand would most probably lead to a deepening of the central valley rather than a splitting into a series of branches as interpreted by Urien and Ottmann (1971).

Depocenter shifts and transport pathways

As sea level determines the framing conditions for depocenter formation, the following discussion is subdivided into time intervals according to the major sea-level stages. The individual sedimentary units are arranged according to the two major sediment sources (i.e., Plata and Argentine provinces) to reveal the specific transport pathways and depocenter formation history.

MIS 3 (60–26.5 cal ka BP)

The sediment dispersal during MIS 3 (Fig. 9) is based on the assumption that the Plata remained the course towards the north and did not switch its central valley (see section "The course of the Plata River since the LGM"). U8 represents the main shelf depocenter for Plata fines during MIS 3 (Fig. 8). U8 is not restricted to the northward located Plata mouth and, therefore, a secondary southward transport of these fines is required for the formation of the wide U8 deposits. A possible transport mechanism was the entrainment of fines from the Plata plume into the southward flowing STSW (Fig. 9). The maximum southward extent of the STSW and, thus, the latitudinal STSF location mainly depend on the barotropic pressure gradient set-up by the northernmost extent of the MC (Palma et al., 2008). The strength of this pressure gradient is mainly determined by the shelf width (Csanady, 1978). Under present-day conditions the STSF shows a maximum northward extension of about 600 km to the northeast of the MC's northernmost expansion limit (Piola et al., 2008). A narrower shelf during lower sea levels would result in a southward STSF displacement. In the extreme case of a very narrow shelf (i.e., during LGM), the STSF was most probably located at a similar latitude as the MC's northernmost penetration. Such STSF displacement south of the Uruguayan sector would favor a southward advective transport of Plata fines in the study area. Positions south of the STSF would remain bare of U8 sediments. Indeed, in our acoustic profiles U8 sediments are absent south of 36°S. Therefore, the main controlling factor for the deposition of U8 was the material transport by shelf currents.

The contourite drift NTD predominately received material from the Argentine margin (Figs. 8 and 9) as a consequence of a continuous redeposition and northward material transport by water masses. However, provenance analysis indicates minor but persistent contribution of Plata-derived material. Due to the northern location of the Plata mouth during times of lower sea level, material transport from the Plata province towards the NTD must have occurred through a southward-flowing water mass. In the modern situation, the only water

https://doi.org/10.1016/j.yqres.2014.01.003 Published online by Cambridge University Press

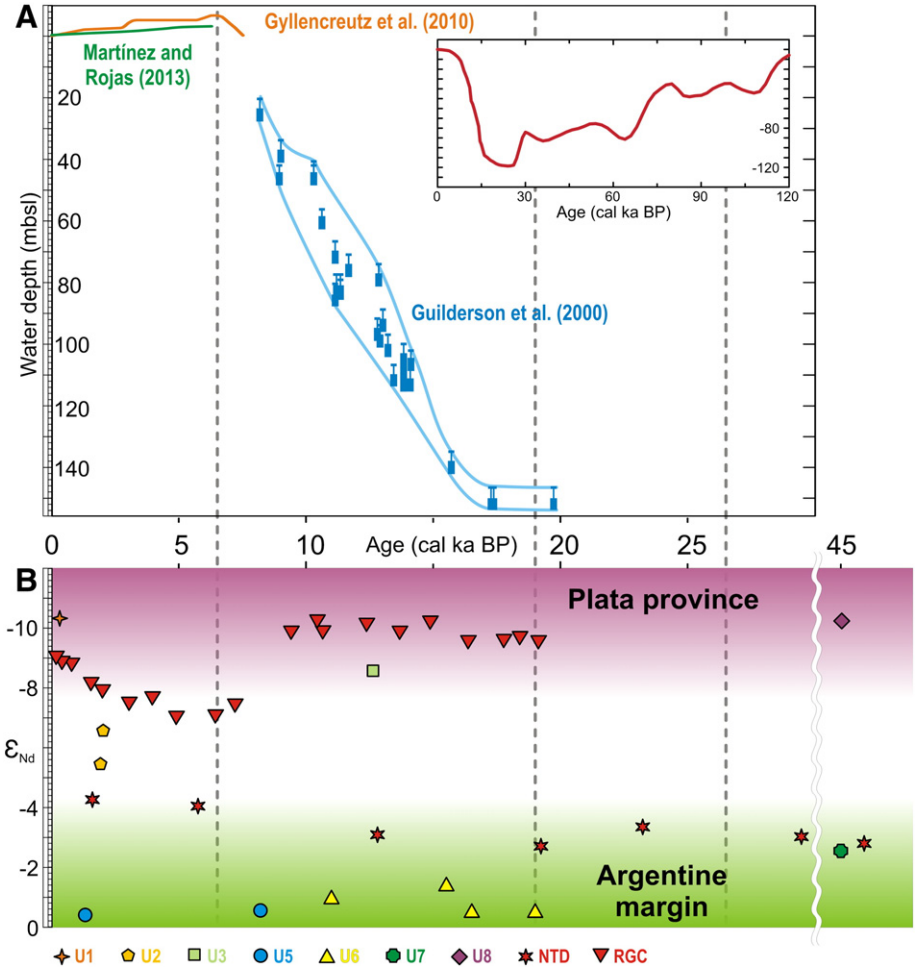

Figure 8. (A) Relative sea-level curves from SE South America (mbsl = meters below modern sea level). The relative sea-level curve from Gyllencreutz et al. (2010) is based on data from Cavallotto et al. (2004). Data from Guilderson et al. (2000) are displayed as boxes with error bars. Inset shows the eustatic sea-level reconstruction by Peltier and Fairbanks (2006) of the past 120 ka. (B) Nd-isotope measurements of the sedimentary units. Sediment sources "Plata province" and "Argentine margin" are based on the subdivision of Mahiques et al. (2008). Please see Table 2 for εNd values and the age of the displayed samples.

masses at the continental slope fulfilling this requirement are the recirculated AAIW and the NADW (Georgi, 1981; Saunders and King, 1995; Piola and Matano, 2001; Carter and Cortese, 2009). The recirculated AAIW, however, is not expanding south of the BMC. Therefore, particles from the Plata province are most likely transported southward by the NADW where they contribute the formation of the NTD (Fig. 9). During MIS3 the stratification of intermediate and deep-water masses for the western South Atlantic remains elusive due to the lack of detailed information. Thus, one may assume that MIS 3 experienced a similar water-mass stratification as the one suggested for the LGM. It has been proposed that the core of the glacial counterpart of NADW, known as Glacial North Atlantic Intermediate Water (GNAIW), was centered at a shallower depth (i.e., 1500 m vs. modern 2500 m water depth; Marchitto et al., 1998; Curry and Oppo, 2005). Though shallower, the GNAIW could have transported a fraction of Plata-derived material during MIS 3 and the LGM.

The shoreface deposits of U7 are composed of Argentine margin sands. The progradation of U7 from mid-shelf towards outer shelf was directly linked to the shore migration during the last major sea-level regression. A falling base level and associated lowering of the wave base led to the formation of a regressive surface of marine erosion sensu Catuneanu et al. (2011). Then, redeposited sediments from the Argentine province prograded across this surface. Direct fluvial supply by the Plata was absent (Fig. 8). Hence, the U7 shoreface sediments stemmed from alongshore transport and erosion of older shelf deposits.

Full-glacial sea-level lowstand (26.5–19 cal ka BP)

During LGM, major parts of the shelf were exposed and the Plata River mouth reached its northernmost position (e.g., Urien et al., 1980a; Cavallotto and Violante, 2005). The close proximity of the Plata mouth to RGC at that time and the high sedimentation rates of about 250 cm ka^{-1} (Fig. 7) indicate direct and strong supply of Plata fines to the cone (Fig. 9). Therefore, RGC was the main sink for Plata-derived sediments during LGM (Figs. 8 and 9).

NTD and U6 were the main depocenters for material from the Argentine margin during LGM. The contourite drift NTD formed at the LCDW-AABW boundary due to the associated turbulent energy (Preu et al., 2013). The provenance of NTD sediments indicates no significant changes compared to MIS 3. Earliest U6 deposition on the shelf formed shoreface deposits in association with the initiation of sea-level rise. The absence of any major progradational outer-shelf deposit during the LGM contrasts the existence of river-related lowstand deltas as formerly proposed by Urien and Ottmann (1971) and Martins et al. (2005).

Deglacial and early Holocene sea-level rise (19–6.5 cal ka BP)

RGC, U4, and U3 were the main depocenters for Plata fines during the deglacial period and early Holocene sea-level rise. The landward shift of the coastline during rising sea level is mirrored by a drastically decreasing sedimentation rate at the RGC (Fig. 7). Nevertheless, RGC provenance shows dominant Plata material supply until at least

https://doi.org/10.1016/j.yqres.2014.01.003 Published online by Cambridge University Press

9.5 cal ka BP (Fig. 8). Afterwards, a significant contribution of sandy material from the Argentine margin occurred until about 5 cal ka BP. Such a coarsening trend is corroborated by other studies and was related to: (1) low terrigenous supply due to a reduced Plata discharge (Mahiques et al., 2009), (2) trapping of fine sediments in the Plata Estuary and increased northward transport of coarse sediments from the Argentine shelf by strong wind-driven coastal currents (Gyllencreutz et al., 2010), and (3) an SASW strengthening displacing the STSF northward (Razik et al., 2013). The first option is corroborated by the reconstruction of dry climate conditions during the mid-Holocene in the Plata drainage basin (e.g., Cruz et al., 2005). However, decreased terrigenous supply could have led to a decreased Plata provenance signal but would have been accompanied by a decrease in sedimentation rate of RGC. As this is not the case during the Holocene, a northward displacement of the STSF explains both increased contribution of Argentine margin material and coarser grain size of RGC after ~9.5 cal ka BP (Fig. 9). An increased strength of the coastal current system might have contributed the northward transport of Argentine sands but a direct effect on RGC formation remains speculative.

The initial deposition of the incised valley fills of U4 and of the tidal U3 started probably with the early flooding of the outer Plata paleovalley. This idea is corroborated by rapidly decreasing sedimentation rates within RGC during early deglacial times (Fig. 7). Thus, the U3 deposits found at the inner shelf provide a snapshot of the generally landward migration of facies zones during deglacial sea-level rise. This landward shift continued probably until ~6.5 cal ka BP when the regional sea level arrived at its highstand (Gyllencreutz et al., 2010; Fig. 9).

Main deglacial depocenters composed of sands from the Argentine province are NTD, U6, and U5. NTD shows a decreasing sedimentation rate during rapidly rising sea level (Fig. 7) probably due to enhanced material retention on the progressively flooded shelf. Furthermore, the distribution of water masses had probably an influence on the sedimentation rate. It was suggested that NTD had formed at the LCDW-AABW interface during LGM and that this interface shifted downwards during deglaciation placing NTD into the sole influence of the LCDW (Preu et al., 2013). This downward shift would have resulted in a less energetic depositional environment and, therefore, a decreased contribution of redeposited material to the location of the NTD. An alternative explanation for a relatively stronger Plata province influence would be a higher contribution of Plata fines by a strengthening of the NADW, which was observed by, for example, Oppo and Fairbanks (1987) and Viana et al. (2002).

The distribution of U6 and U5 reveals that deglacial deposits receiving Argentine margin material showed a wider distribution on the continental shelf compared to the deposition of Plata fines, which were restricted to the paleo-valley (Fig. 9). After initial formation of U6 during LGM, the zone of active fine sandy to gravelly shoreface deposition migrated landward along with the drowning of the shelf. Hence, the main controls on the formation of U6 were the rising sea level and the influence of waves on the shoreface sedimentation. The confined deposition and the absence of a widespread sediment drape point to prevailing strong hydrodynamic conditions. The transition from fine sands and gravels (U6) towards muddy very fine sandy depression fills (U5) indicates a trend towards overall calmer conditions due to an upward shift of the wave base during deglacial sea-level rise. The sediment provenance of U5 points to a supply of material from the Argentine margin by shelf water masses (Figs. 9). The transport of very fine sands by shelf water masses is indicated by the observation that the deposition of U5 is still active today and that large amounts of sands are exported across the shelf edge (Bender et al., 2013). One of the few direct current velocity measurement on the shelf off SE South America was carried out by Zavialov et al. (2002). Current velocities are highly variable but peaks stronger than 50 cm s^{-1} were recorded about 10 m above the bottom. Hence, the bottom velocities should be strong enough to transport very fine sands (Sundborg, 1956). Studies on the more complex interaction of factors such as near-bed current velocity, shear stress, and turbulence in the bottom boundary layer are not available off SE South America. However, another indication for a strong current regime is the absence of muddy surface sediment on major parts of the shelf (e.g., Urien et al., 1980a).

Mid-Holocene sea-level highstand and late Holocene sea-level fall (6.5–0 cal ka BP)

The maximum flooding of the Plata Estuary occurred with the mid-Holocene sea-level highstand at 6.5 cal ka BP (Gyllencreutz et al.,

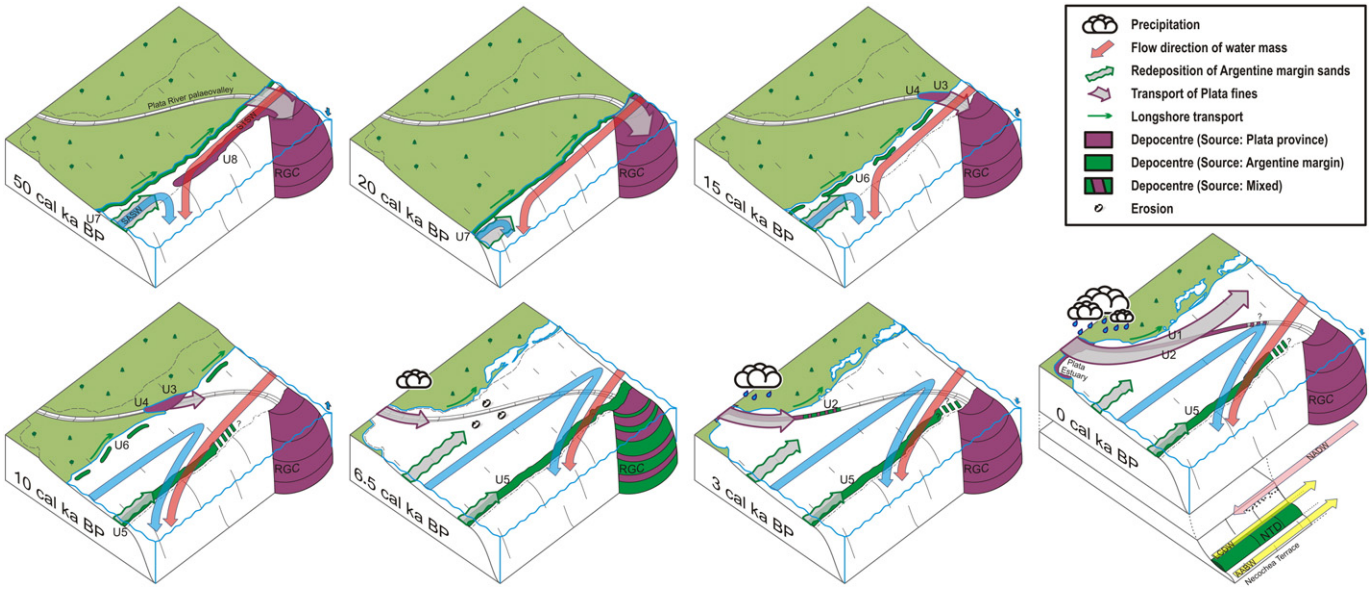

Figure 9. Schematic block diagram showing the sedimentary evolution of the SE South American margin within time slices. The evolution of the displayed lagoons is based on Villwock (1984) and Cordeiro and Lorscheitter (1994). Water masses (PPW = Plata Plume Water; SASW = Subantarctic Shelf Water; STSW = Subtropical Shelf Water) are displayed as arrows based on Piola et al. (2008) and Hernández-Molina et al. (2009). The modern time slice additionally displays depocenter NTD and water masses at the lower slope (NADW = North Atlantic Deep Water; LCDW = Lower Circumpolar Deep Water; AABW = Antarctic Bottom Water). Locations and shifts of the water masses within the displayed time slices are discussed in the text. Mid- to late Holocene increase of precipitation (displayed by rain clouds) is based on the studies of Behling et al. (2004), Bracco et al. (2005), Cruz et al. (2005, 2007), and Mahiques et al. (2009). Glacial to early Holocene precipitation values are under debate (e.g., Behling et al., 2004; Vimeux et al., 2009) and are, therefore, not displayed.

https://doi.org/10.1016/j.yqres.2014.01.003 Published online by Cambridge University Press

2010) coinciding with the northernmost location of the STSF (Razik et al., 2013). After a gradual fall towards the modern sea-level position (Martínez and Rojas, 2013), the present distribution of shelf water masses was established (Gyllencreutz et al., 2010; Razik et al., 2013).

Fine sediments discharged from the Plata region are believed to have been mainly trapped within the estuary until ~5 cal ka BP (Gyllencreutz et al., 2010). Indeed, the sedimentation rate of Plata-derived material within RGC decreased remarkably during the deglacial flooding of the shelf (Fig. 7), and deposits on the outer shelf (U5) did not receive any Plata-derived material (Fig. 8). Nevertheless, RGC provenance shows a reduced but persistent supply of these fines to the Rio Grande Cone (Figs. 7 and 8). In addition, NTD sediments reveal a shift from a pure Argentine signature towards a mixed signal, i.e. higher contribution of Plata fines after ~12 cal ka BP (Fig. 8), which points towards the aforementioned strengthening of the NADW. The strongest contribution of Argentine sands to RGC was recorded around 6.5 to 5 cal ka BP leading to a mixed source signature (Fig. 8). This increased contribution was most probably related to the northernmost displacement of the STSF. On the Brazilian shelf the transport of Argentine sands during this time interval reached at least up to 25°S (Gyllencreutz et al., 2010).

Coinciding with this time interval of northernmost transport of Argentine sands, an erosional surface developed inside the Plata paleo-valley, prior to the initial deposition of U2 at around 4.6 cal ka BP. The onset of the locally confined sand body U2 above this surface indicates decreased hydrodynamic energy enabling the deposition of this material on the shelf (Fig. 9). The basal age of U2 coincides with the decreasing Argentine material content at the RGC (Fig. 8). Furthermore, deposits located off SE Brazil show a prominent fining at around 5 cal ka BP (Mahiques et al., 2009; Gyllencreutz et al., 2010). While Mahiques et al. (2009) related this shift to a decreasing terrigenous supply, Gyllencreutz et al. (2010) proposed an increase of the Plata discharge blocking the SASW and, therefore, hindering Argentine sands to be transported farther northwards. According to the reconstruction of Razik et al. (2013), the STSF was in the process of shifting southward from its northernmost position during the mid-Holocene to its modern location. The two latter options imply a relative weakening of the SASW leading to a decreasing current strength on the shelf, which led to the initial formation of U2. The paleo-valley provided a sheltered position to deposit these sediments. A part of the Plata fines got entrained into U2 leading to a mixed εNd-signature (Fig. 8), which documents an increased export of fluvial suspended sediments. On the one hand, the available accommodation space of most estuaries was largely re-filled between ~7.8 and ~4.4 cal ka BP, which resulted in increased material export to the shelf (Long, 2001). On the other hand, paleo-climate reconstructions showed that the change from arid conditions towards the present wet climate within the Plata catchment area occurred during the late Holocene (Marchant and Hooghiemstra, 2004; Bracco et al., 2005; Baker et al., 2009; Behling and Safford, 2010). As a consequence, the export of fines from the Plata Estuary should have gradually increased (Fig. 9).

The remarkably high sedimentation rate of the relatively modern mud depocenter U1 reflects the strong terrigenous supply by the Plata Estuary. Therefore, the onset of U1 at ~1.5 cal ka BP should be connected to changes in the Plata drainage basin. Behling et al. (2004), Cruz et al. (2007), and Mahiques et al. (2009) described increasing precipitation in the Paraná catchment area (S Brazil) for the past 2 cal ka BP and Bracco et al. (2005) showed humid conditions having established after 1.7 cal ka BP. The change towards higher precipitation led to an increased Plata discharge and, consequently, stronger export of fine material to the shelf (Fig. 9). Despite the increased export of Plata fines, the transformation from sand (U2) to mud (U1) deposition required a further weakening of the shelf current regime, most probably related to the further southward shift of the STSF towards its modern position (Fig. 9).

Conclusions

Coarse-grained material from the Argentine margin is distributed by extensive redeposition due to the persistent strong current regime and was deposited in the form of: (1) long-lasting contourite drift deposits at the northern Argentine continental slope, (2) sandy regressive shoreface deposits on the mid- and outer shelf, (3) local transgressive shelf sand bodies, (4) muddy depression fills and drapes covering the wavy outer-shelf morphology during the late stage of sea-level rise, and (5) a local Holocene sand body within the La Plata River paleo-valley.

Fine-grained sediments delivered by the La Plata River show completely different dispersal patterns. During most parts of the sea-level cycle these fines were transported northwards along the La Plata River paleo-valley, which acted as the sole transit way for the huge volumes of fluvially supplied fines during intervals of lower sea level. Material supplied by the La Plata River formed as main depocenters: (1) an aggradational mud deposit at the outermost shelf dating into MIS 3, (2) the Rio Grande Cone at the continental slope, mainly active during the last glacial maximum, and (3) a tidal to open-marine succession related to the drowning of the La Plata River paleo-valley on the inner shelf since deglacial times.

Although large volumes of sediments were persistently contributed from the major fluvial supplier as well as from the southerly located wide shelf, strong currents prevented thick and extensive sediment accumulation on the shelf during any time of the past sea-level cycle. Deposition was restricted to (1) shoreface environments, (2) the La Plata River paleo-valley, and (3) deeper waters of the outer shelf. Hence, current strength played the crucial role in distributing sediments and, therefore, the shelf off the La Plata Estuary can be considered as a hydrodynamically controlled end-member.

Acknowledgments

Radiocarbon ages of Core GeoB13802-2 were kindly provided by André Klicpera (Dept. of Biogeochemistry / Geology at the Leibniz Center for Tropical Marine Ecology, Bremen). We are thankful to Derek Vance for Nd-isotope measurements. We also wish to thank Alberto Piola and Benedict Preu for their helpful comments on the oceanography of the region. Special thanks go to Captain and crew of RV Meteor during cruise M78-3 for their outstanding support. The study was funded through DFG-Research Center/Cluster of Excellence "The Ocean in the Earth System". Till Hanebuth acknowledges a Heisenberg fellowship (HA4217/4-1). Cristiano M. Chiessi acknowledges the financial support from FAPESP (grants 2010/09983-9 and 2012/17517-3). We also wish to thank Rüdiger Henrich for providing laboratory facilities. This paper was improved by helpful comments from the two anonymous reviewers. The data reported in this paper will be archived in Pangaea (www.pangaea.de).

References

Ayup, R.N., 1987. Intercâmbio Sedimentar entre o Río de La Plata Exterior e a Plataforma Continental Adjacente. Pesquisas 19, 105–126.

Baker, P.A., Fritz, S.C., Burns, S.J., Ekdahl, E., Rigsby, C.A., 2009. The nature and origin of decadal to millennial scale climate variability in the southern tropics of South America: the Holocene record of Lago Umayo, Peru. In: Vimeux, F., Sylvestre, F., Khodri, M. (Eds.), Past Climate Variability in South America and Surrounding Regions. Springer, pp. 301–322.

Behling, H., Safford, H.D., 2010. Late-glacial and Holocene vegetation, climate and fire dynamics in the Serra dos Órgãos, Rio de Janeiro State, southeastern Brazil. Global Change Biology 16 (6), 1661–1671.

Behling, H., Pillar, V.D., Orloic, L., Bauermann, S.G., 2004. Late Quaternary Araucaria forest, grassland (Campos), fire and climate dynamics, studied by high-resolution pollen, charcoal and multivariate analysis of the Cambara do Sul core in southern Brazil. Palaeogeography, Palaeoclimatology, Palaeoecology 203 (3–4), 277–297.

Bender, V., Hanebuth, T.J.J., Chiessi, C.M., 2013. Holocene shifts of the Subtropical Shelf Front off southeastern South America controlled by high and low latitude forcing. Paleoceanography 28 (1–10). http://dx.doi.org/10.1002/palo.20044.

Blair, T.C., McPherson, J.G., 1999. Grain-size and textural classification of coarse sedimentary particles. Journal of Sedimentary Research 69 (1), 6–19.
Bleil, U. and cruise participants, 2001. Geo Bremen South Atlantic 1999/2000, Part 3, Cruise No. 46, Leg 3, Montevideo–Mar del Plata, 4 January–7 February 2000. Meteor-Berichte 01-1.
Bracco, R., Inda, H., del Puerto, L., Castiñeira, C., Sprechmann, P., García-Rodríguez, F., 2005. Relationships between Holocene sea-level variations, trophic development, and climatic change in Negra Lagoon, Southern Uruguay. Journal of Paleolimnology 33 (3), 253–263.
Carter, L., Cortese, G., 2009. Change in the Southern Ocean: responding to Antarctica. In: Brigham-Grette, J., Powell, R., Newman, L., Kiefer, T. (Eds.), PAGES News: Change at the Poles, A Paleoscience Perspective. PAGES International Project Office, pp. 30–32.
Castillo, L.A.L., Kazmierczak, T.D., Chemale, F., 2009. Rio Grande Cone tectono-stratigraphic model — Brazil: seismic sequences. Earth Sciences Research Journal 13 (1), 42–53.
Catuneanu, O., Galloway, W.E., Kendall, C.G.S.t.C., Miall, A.D., Posamentier, H.W., Strasser, A., Tucker, M.E., 2011. Sequence stratigraphy: methodology and nomenclature. Newsletters on Stratigraphy 44 (3), 173–245.
Cavallotto, J.L., Violante, R.A., 2005. Geología y Geomorfología del Río de la Plata. In: De Barrio, R., Etcheverry, R.O., Caballé, M.F., Llambías, E. (Eds.), Geología y recursos minerales de la Provincia de Buenos Aires. Relatorio XVI Congreso Geológico Argentino, La Plata, Cap. XIV, pp. 237–253.
Cavallotto, J.L., Violante, R.A., Parker, G., 2004. Sea-level fluctuations during the last 8600 years in the de la Plata river (Argentina). Quaternary International 114 (1), 155–165.
Cawthra, H.C., Neumann, F.H., Uken, R., Smith, A.M., Guastella, L.A., Yates, A., 2012. Sedimentation on the narrow (8 km wide), oceanic current-influenced continental shelf off Durban, Kwazulu-Natal, South Africa. Marine Geology 323–325 (0), 107–122.
Chiessi, C.M., Mulitza, S., Paul, A., Pätzold, J., Groeneveld, J., Wefer, G., 2008. South Atlantic interocean exchange as the trigger for the Bølling warm event. Geology 36 (12), 919–922.
Cordeiro, S., Lorscheitter, M., 1994. Palynology of Lagoa dos Patos sediments, Rio Grande do Sul, Brazil. Journal of Paleolimnology 10 (1), 35–42.
Cruz, F.W., Burns, S.J., Karmann, I., Sharp, W.D., Vuille, M., Cardoso, A.O., Ferrari, J.A., Dias, P.L.S., Viana, O., 2005. Insolation-driven changes in atmospheric circulation over the past 116,000 years in subtropical Brazil. Nature 434 (7029), 63–66.
Cruz, F.W., Burns, S.J., Jercinovic, M., Karmann, I., Sharp, W.D., Vuille, M., 2007. Evidence of rainfall variations in Southern Brazil from trace element ratios (Mg/Ca and Sr/Ca) in a Late Pleistocene stalagmite. Geochimica et Cosmochimica Acta 71 (9), 2250–2263.
Csanady, G.T., 1978. The arrested topographic wave. Journal of Physical Oceanography 8 (1), 47–62.
Curry, W.B., Oppo, D.W., 2005. Glacial water mass geometry and the distribution of δ13C of ΣCO2 in the western Atlantic Ocean. Paleoceanography 20 (1), PA1017. http://dx.doi.org/10.1029/2004pa001021.
Depetris, P.J., Griffin, J.J., 1968. Suspended load in Rio de la Plata drainage basin. Sedimentology 11 (1–2), 53–60.
Ewing, M., Lonardi, A.G., 1971. Sediment transport and distribution in the Argentine Basin. 5. Sedimentary structure of the Argentine margin, basin, and related provinces. Physics and Chemistry of the Earth 8, 123–251.
Flemming, B.W., 1981. Factors controlling shelf sediment dispersal along the southeast African continental margin. Marine Geology 42 (1–4), 259–277.
Fontana, R., 1996. Geotectônica e sismoestratigrafia da Bacia de Pelotas e Plataforma de Florianópolis. (Ph.D. thesis) Universidade Federal do Rio Grande do Sul.
García-Rodríguez, F., Metzeltin, D., Sprechmann, P., Trettin, R., Stams, G., Beltrán-Morales, L.F., 2004. Upper Pleistocene and Holocene paleosalinity and trophic state changes in relation to sea level variation in Rocha Lagoon, southern Uruguay. Journal of Paleolimnology 32 (2), 117–135.
General Bathymetric Chart of the Oceans (GEBCO), 2008. http://www.gebco.net.
Georgi, D.T., 1981. On the relationship between the large-scale property variations and fine structure in the circumpolar deep water. Journal of Geophysical Research 86 (C7), 6556–6566.
Goldstein, S.L., O'Nions, R.K., Hamilton, P.J., 1984. A Sm–Nd isotopic study of atmospheric dusts and particulates from major river systems. Earth and Planetary Science Letters 70 (2), 221–236.
Guerrero, R.A., Acha, E.M., Framinan, M.B., Lasta, C.A., 1997. Physical oceanography of the Río de la Plata Estuary, Argentina. Continental Shelf Research 17 (7), 727–742.
Guilderson, T.P., Burckle, L., Hemming, S., Peltier, W.R., 2000. Late Pleistocene sea level variations derived from the Argentine Shelf. Geochemistry, Geophysics, Geosystems 1 (12), 1055. http://dx.doi.org/10.1029/2000GC000098.
Gwilliam, C.S., Coward, A.C., de Cuevas, B.A., Webb, D.J., Rourke, E., Thompson, S.R., Döös, K., 1997. The OCCAM global model. In: García, F.G., Cisneros, G., Fernández, A.E., Álvarez, R. (Eds.), Numerical Simulations in the Environmental and Earth Sciences: Proceedings of the Second UNAM-CRAY Supercomputing Conference. Cambridge University Press, p. 299.
Gyllencreutz, R., Mahiques, M.M., Alves, D.V.P., Wainer, I.K.C., 2010. Mid- to late-Holocene paleoceanographic changes on the southeastern Brazilian shelf based on grain size records. Holocene 20 (6), 863–875.
Hanebuth, T.J.J., Stattegger, K., Bojanowski, A., 2009. Termination of the last glacial maximum sea-level lowstand: the Sunda-Shelf data revisited. Global and Planetary Change 66 (1–2), 76–84.
Hanebuth, T.J.J., Voris, H.K., Yokoyama, Y., Saito, Y., Okuno, J.i, 2011. Formation and fate of sedimentary depocenters on Southeast Asia's Sunda Shelf over the past sea-level cycle and biogeographic implications. Earth-Science Reviews 104 (1–3), 92–110.
Harris, P.T., Whiteway, T., 2011. Global distribution of large submarine canyons: geomorphic differences between active and passive continental margins. Marine Geology 285 (1–4), 69–86.
Hernández-Molina, F.J., Paterlini, M., Violante, R., Marshall, P., de Isasi, M., Somoza, L., Rebesco, M., 2009. Contourite depositional system on the Argentine Slope: an exceptional record of the influence of Antarctic water masses. Geology 37 (6), 507–510.
Hübscher, C., Figueiredo, A.G., Kruse, L., Spieß, V., 2002. High-resolution analysis of the deposition pattern on the Amazon sub-aquatic delta and outer continental shelf. Marine Geophysical Researches 23 (3), 209–222.
Ikehara, K., 1989. The Kuroshio-generated bedform system in the Osumi Strait, Southern Kyushu, Japan. In: Taira, A., Masuda, F. (Eds.), Sedimentary Facies in the Active Plate Margin. Terra Scientific Publishing Company, Tokyo, pp. 261–273.
Innocent, C., Fagel, N., Hillaire-Marcel, C., 2000. Sm–Nd isotope systematics in deep-sea sediments: clay-size versus coarser fractions. Marine Geology 168 (1–4), 79–87.
Krastel, S. and cruise participants, 2012. Sediment transport off Uruguay and Argentina: From the shelf to the deep sea. 19.05.2009–06.07.2009, Montevideo (Uruguay) – Montevideo (Uruguay). Berichte, Fachbereich Geowissenschaften, Universität Bremen 285.
Kuehl, S.A., Levy, B.M., Moore, W.S., Allison, M.A., 1997. Subaqueous delta of the Ganges-Brahmaputra river system. Marine Geology 144 (1–3), 81–96.
Laborde, J.L., 1999. Sand deposits of the outer Río de la Plata and adjacent continental shelf. In: Martins, L.R., Santana, C.I. (Eds.), Non Living Resources of the Southern Brazilian Coastal Zone and Continental Margin.
Laskar, J., Robutel, P., Joutel, F., Gastineau, M., Correia, A.C.M., Levrard, B., 2004. A long-term numerical solution for the insolation quantities of the Earth. Astronomy & Astrophysics 428 (1), 261–285.
Lonardi, A.G., Ewing, M., 1971. Sediment transport and distribution in the Argentine Basin. 4. Bathymetry of the continental margin, Argentine Basin and other related provinces. Canyons and sources of sediments. Physics and Chemistry of the Earth 8, 79–121.
Long, A., 2001. Mid-Holocene sea-level change and coastal evolution. Progress in Physical Geography 25 (3), 399–408.
Mahiques, M.M., Tassinari, C.C.G., Marcolini, S., Violante, R.A., Figueira, R.C.L., da Silveira, I.C.A., Burone, L., de Mello e Sousa, S.H., 2008. Nd and Pb isotope signatures on the Southeastern South American upper margin: implications for sediment transport and source rocks. Marine Geology 250 (1–2), 51–63.
Mahiques, M.M., Coaracy Wainer, I.K., Burone, L., Nagai, R., de Mello e Sousa, S.H., Lopes Figueira, R.C., Almeida da Silveira, I.C., Bícego, M.C., Vicente Alves, D.P., Hammer, Ø., 2009. A high-resolution Holocene record on the Southern Brazilian shelf: paleoenvironmental implications. Quaternary International 206 (1–2), 52–61.
Marchant, R., Hooghiemstra, H., 2004. Rapid environmental change in African and South American tropics around 4000 years before present: a review. Earth-Science Reviews 66 (3–4), 217–260.
Marchitto, T.M., Curry, W.B., Oppo, D.W., 1998. Millennial-scale changes in North Atlantic circulation since the last glaciation. Nature 393 (6685), 557–561.
Martínez, S., Rojas, A., 2013. Relative sea level during the Holocene in Uruguay. Palaeogeography, Palaeoclimatology, Palaeoecology 374, 123–131.
Martins, L.R., Corrêa, I.C.S., 1996. Atlas Morphology and Sedimentology of the Southwest Atlantic Coastal Zone and Continental Shelf from Cabo Frio (Brazil) and Peninsula Valdés (Argentina). Universidade Federal do Rio Grande do Sul, Brazil.
Martins, L.R., Urien, C.M., Martins, I.R., 2005. Gênese dos Sedimentos da Plataforma Continental Atlântica entre o Rio Grande do Sul (Brasil) e Tierra del Fuego (Argentina). Gravel 3, 85–102.
Milliman, J.D., Farnsworth, K.L., 2011. River Discharge to the Coastal Ocean: A Global Synthesis. Cambridge University Press, Cambridge.
Möller, O.O., Piola, A.R., Freitas, A.C., Campos, E.J.D., 2008. The effects of river discharge and seasonal winds on the shelf off southeastern South America. Continental Shelf Research 28 (13), 1607–1624.
Oppo, D.W., Fairbanks, R.G., 1987. Variability in the deep and intermediate water circulation of the Atlantic Ocean during the past 25,000 years: Northern Hemisphere modulation of the Southern Ocean. Earth and Planetary Science Letters 86 (1), 1–15.
Palma, E.D., Matano, R.P., Piola, A.R., 2008. A numerical study of the Southwestern Atlantic Shelf circulation: stratified ocean response to local and offshore forcing. Journal of Geophysical Research 113 (C11), C11010.
Parker, G., Violante, R.A., Paterlini, C.M., Costa, I.P., Marcolini, S.I., Cavallotto, J.L., 2008. Las Secuencias Depositacionales del Plioceno-Cuaternario en la Plataforma Submarina adyacente al Litoral del Este Bonaerense. Latin American Journal of Sedimentology and Basin Analysis 15 (2), 105–124.
Peltier, W.R., Fairbanks, R.G., 2006. Global glacial ice volume and Last Glacial Maximum duration from an extended Barbados sea level record. Quaternary Science Reviews 25 (23–24), 3322–3337.
Piola, A.R., Matano, R.P., 2001. Brazil and Falklands (Malvinas) Currents. In: John, H.S., Karl, K.T., Steve, A.T. (Eds.), Encyclopedia of Ocean Sciences. Academic Press, Oxford, pp. 340–349.
Piola, A.R., Campos, E.J.D., Möller Jr., O.O., Charo, M., Martinez, C., 2000. Subtropical Shelf Front off eastern South America. Geophysical Research Letters 105 (C3), 6565–6578.
Piola, A.R., Möller Jr., O.O., Guerrero, R.A., Campos, E.J.D., 2008. Variability of the subtropical shelf front off eastern South America: winter 2003 and summer 2004. Continental Shelf Research 28 (13), 1639–1648.
Preu, B., Schwenk, T., Hernández-Molina, F.J., Violante, R., Paterlini, M., Krastel, S., Tomasini, J., Spieß, V., 2012. Sedimentary growth pattern on the northern Argentine slope: the impact of North Atlantic Deep Water on southern hemisphere slope architecture. Marine Geology 329–331, 113–125.
Preu, B., Hernández-Molina, F.J., Violante, R., Piola, A.R., Paterlini, C.M., Schwenk, T., Voigt, I., Krastel, S., Spiess, V., 2013. Morphosedimentary and hydrographic features of the northern Argentine margin: the interplay between erosive, depositional and gravitational processes and its conceptual implications. Deep Sea Research Part I: Oceanographic Research Papers 75, 157–174.
Razik, S., Chiessi, C.M., Romero, O.E., von Dobeneck, T., 2013. Interaction of the South American Monsoon System and the Southern Westerly Wind Belt during the last 14 kyr. Palaeogeography, Palaeoclimatology, Palaeoecology 374, 28–40.

https://doi.org/10.1016/j.yqres.2014.01.003 Published online by Cambridge University Press

Reimer, P.J., Baillie, M.G.L., Bard, E., Bayliss, A., Beck, J.W., Blackwell, P.G., Ramsey, C.B., Buck, C.E., Burr, G.S., Edwards, R.L., Friedrich, M., Grootes, P.M., Guilderson, T.P., Hajdas, I., Heaton, T.J., Hogg, A.G., Hughen, K.A., Kaiser, K.F., Kromer, B., McCormac, F.G., Manning, S.W., Reimer, R.W., Richards, D.A., Southon, J.R., Talamo, S., Turney, C.S.M., van der Plicht, J., Weyhenmeyer, C.E., 2009. IntCal09 and Marine09 radiocarbon age calibration curves, 0–50,000 years cal BP. Radiocarbon 51 (4), 1111–1150.

Revel, M., Cremer, M., Grousset, F.E., Labeyrie, L., 1996. Grain-size and Sr–Nd isotopes as tracer of paleo-bottom current strength, Northeast Atlantic Ocean. Marine Geology 131 (3–4), 233–249.

Sato, K., Tassinari, C.C.G., Kawashita, K., Petronilho, L., 1995. A metodologia Sm–Nd no IGc-USP e suas aplicações. Anais da Academia Brasileira de Ciências 67, 313–336.

Saunders, P.M., King, B.A., 1995. Oceanic fluxes on the WOCE A11 section. Journal of Physical Oceanography 25 (9), 1942–1958.

Schulz, H.D. and cruise participants, 2001. Geo Bremen South Atlantic 1999/2000, Part 2, Cruise No. 46, Leg 2, Recife-Montevideo, 2–29 December 1999. Meteor-Berichte 01-1.

Stoll, H.M., Vance, D., Arevalos, A., 2007. Records of the Nd isotope composition of seawater from the Bay of Bengal: implications for the impact of Northern Hemisphere cooling on ITCZ movement. Earth and Planetary Science Letters 255 (1–2), 213–228.

Stuiver, M., Reimer, P.J., Bard, E., Beck, J.W., Burr, G.S., Hughen, K.A., Kromer, B., McCormac, G., Van der Plicht, J., Spurk, M., 1998. INTCAL98 radiocarbon age calibration, 24,000–0 cal BP. Radiocarbon 40 (3), 1041–1083.

Sundborg, Å., 1956. The river Klarälven. A study of fluvial processes. Geografiska Annaler 38, 127–316.

Tossini, L., 1959. El sistema hidrográfico de la Cuenca del Rio de la Plata. Anales de la Sociedad Cientifica Argentina 167, 41–64.

Urien, C.M., 1972. Rio de la Plata estuary environments. Geological Society of America Memoir 133, 213–234.

Urien, C.M., Ewing, M., 1974. Recent sediments and environment of southern Brazil, Uruguay, Buenos Aires, and Rio Negro continental shelf. In: Burk, C.A., Drake, C.L. (Eds.), The Geology of Continental Margins. Springer, New York, pp. 157–177.

Urien, C.M., Ottmann, F., 1971. Histoire du Rio de la Plata au Quaternaire. Quaternaria 14, 51–59.

Urien, C.M., Martins, L.R., Martins, I.R., 1980a. Evolução geológica do Quaternário do litoral atlântico uruguaio, plataforma continental e regiões vizinhas. Notas Técnicas 3, 7–43.

Urien, C.M., Martins, L.R., Martins, I.R., 1980b. Modelos deposicionais na plataforma continental do Rio Grande do Sul (Brasil), Uruguai e Buenos Aires. Notas Técnicas 3, 13–25.

Urien, C.M., Martins, L.R., Cazenave, P., 1995. Late Quaternary geology of the Rio de la Plata, Buenos Aires — Rio Negro coastal plain and continental shelf. Encontro de Geologia do Cone Sul, 1° Resumos Expandidos, pp. 273–274.

Van Wagoner, J.C., Posamentier, H.W., Mitchum, H.W., Vail, P.R., Sarg, J.F., Loutit, T.S., J, H., 1988. An overview of sequence stratigraphy and key definitions. In: Wilgus, C.K., Hastings, B.S., Kendall, C.G.S.C., Posamentier, H.W., Ross, C.A., van Wagoner, J.C. (Eds.), Sea Level Changes — An Integrated Approach. Society of Economic Paleontologists and Mineralogists Special Publications, 42. SEPM, Tulsa, pp. 110–124.

Vance, D., Thirlwall, M., 2002. An assessment of mass discrimination in MC-ICPMS using Nd isotopes. Chemical Geology 185 (3–4), 227–240.

Viana, A.R., Hercos, C.M., Almeida Jr., W., Magalhães, J.L.C., Andrade, S.B., 2002. Evidence of bottom current influence on the Neogene to Quaternary sedimentation along the Northern Campos Slope, SW Atlantic Margin. In: Stow, D.A.V., Pudsey, C.J., Howe, J.A., Faugeres, J.-C., Viana, A.R. (Eds.), Deep-Water Contourite Systems: Modern Drifts and Ancient Series, Seismic and Sedimentary Characteristics. The Geological Society, London, pp. 249–259.

Villwock, J.A., 1984. Geology of the coastal province of Rio Grande do Sul, southern Brazil. Pesquisas 16 (5–50).

Vimeux, F., Sylvestre, F., Khodri, M., 2009. Past Climate Variability in South America and Surrounding Regions. Springer.

Violante, R.A., Paterlini, C.M., Costa, I.P., Hernández-Molina, F.J., Segovia, L.M., Cavallotto, J.L., Marcolini, S., Bozzano, G., Laprida, C., García Chapori, N., Bickert, T., Spiess, V., 2010. Sismoestratigrafía y evolución geomorfológico del Talud Continental adyacente al litoral del este bonaerense, Argentina. Latin American Journal of Sedimentology and Basin Analysis 17 (1), 33–62.

Wefer, G. and cruise participants, 2001. Report and preliminary results of Metor cruise m 46/4, Mar Del Plata (Argentina) – Salvador (Brasil), February 10–March 13, 2000. Berichte, Fachbereich Geowissenschaften, Universität Bremen 173.

Zavialov, P., Möller Jr., O., Campos, E., 2002. First direct measurements of currents on the continental shelf of Southern Brazil. Continental Shelf Research 22 (14), 1975–1986.

https://doi.org/10.1016/j.yqres.2014.01.003 Published online by Cambridge University Press